GEOLOGICA CARPATHICA, OCTOBER 2023, 74, 5, 423–440 https://doi.org/10.31577/GeolCarp.2023.22

Paleomagnetic contribution to resolving the tectonic evolution of the Drina–Ivanjica Unit, Internal Dinarides

MÁTÉ VELKI[1,2,✉], EMŐ MÁRTON[2], VESNA CVETKOV[3] and SZILVIA KÖVÉR[4,5]

[1]ELTE Eötvös Loránd University, Institute of Geography and Earth Sciences, Department of Geophysics and Space Science, Pázmány Péter 1/C, 1117 Budapest, Hungary; ✉velki.mate@gmail.com
[2]SARA, Department of Geophysical Research, Paleomagnetic Laboratory, Columbus 17-23, 1145 Budapest, Hungary
[3]University of Belgrade, Faculty of Mining and Geology, Djusina 7, 11000 Belgrade, Serbia
[4]ELTE Eötvös Loránd University, Institute of Geography and Earth Sciences, Department of Physical and Applied Geology, Pázmány Péter 1/C, 1117 Budapest, Hungary
[5]HUN-REN Institute of Earth Physics and Space Sciences, Csatkai E. 6-8, 9400 Sopron, Hungary

(Manuscript received August 29, 2023; accepted in revised form November 15, 2023; Associate Editor: Igor Broska)

Abstract: The Adria-derived Drina–Ivanjica Unit of the Internal Dinarides represents a composite basement-cover thrust sheet passively carrying obducted Jurassic ophiolites and post-obduction Upper Cretaceous sedimentary rocks, penetrated by post-orogenic Miocene igneous rocks. This study presents the first paleomagnetic results from the Drina–Ivanjica Unit obtained at a total of 34 geographically distributed localities, representing Triassic–Jurassic carbonates, Upper Cretaceous carbonate and flysch successions, as well as Miocene igneous rocks. Paleomagnetic directions for the igneous rocks and the Upper Cretaceous flysch, which had clearly remagnetized during Miocene magmatism, point to a 30° clockwise (CW) rotation, which must have taken place after 20 Ma. This angle perfectly agrees with the earlier-published value for both the Western and Eastern Vardar zones (including the Jadar–Kopaonik thrust sheet, the Sava Zone, and the Cretaceous overstepping sequence of the Eastern Vardar ophiolitic unit), suggesting a coordinated rotation between them and the Drina–Ivanjica Unit. Results of the present study set a younger age constraint (20 Ma) for the commencement of the coordinated CW rotation instead of the previously suggested 23 Ma. The rotation may have connected to the extension induced by the slab rollback of the Carpathians, which was also responsible for the opening of the Pannonian Basin. The paleomagnetic directions for the Cenomanian–Turonian carbonates, which are situated far from the magmatic bodies, are interpreted in terms of a minor counter-clockwise (CCW) rotation taking place before the Miocene CW rotation. The Triassic–Jurassic carbonates of the Drina–Ivanjica Unit have post-tilting magnetizations, which were likely induced by the thermal effect of the obducted ophiolites. The overall mean paleomagnetic direction suggests a rotation of about 50° CCW between 150–20 Ma, which is in line with the well-documented post-150 Ma CCW rotation of the Adriatic microplate.

Keywords: Internal Dinarides, Drina–Ivanjica Unit, paleomagnetism, vertical axis rotations

Introduction

The Dinarides form a SW-vergent fold-and-thrust belt in Southeast Europe that evolved from the complex Mesozoic evolution of the northern branch of the Neotethys Ocean, which separated the Adriatic and European plates. The subsequent deformation connected to the rotation and subduction of the Adriatic microplate and the formation of the Pannonian Basin (Pamić et al. 2002; Karamata 2006; Schmid et al. 2008, 2020; Cvetković et al. 2016; Toljić et al. 2018, 2019). Today, remnants of the Neotethys Ocean occur as large ophiolite thrust sheets, which are underlain with tectono-sedimentary mélanges that are arranged along two major subparallel, NW(NNW)–SE(SSE) trending belts extending from the Pannonian Basin to Greece (Fig. 1; Bernoulli & Laubscher 1972; Schmid et al. 2008; Cvetković et al. 2016; Toljić et al. 2019). The Western Vardar ophiolite belt comprises ophiolites obducted westward onto the eastern passive margin of the Adriatic plate in the Late Jurassic to Early Cretaceous (e.g., Dimo-Lahitte et al. 2001; Schmid et al. 2008, 2020; Borojević-Šoštarić et al. 2012, 2014). The Eastern Vardar ophiolites represent the ophiolites, which were tectonically emplaced eastward above parts of the European margin (Schmid et al. 2008, 2020; Toljić et al. 2018). In the Internal Dinarides, the two belts are separated by the Sava suture zone (Schmid et al. 2008; Ustaszewski et al. 2010) or the Central Vardar Zone (Toljić et al. 2018), which represents the Paleogene suture after the closure of the remnant Neotethys and mark the final collision of Adria with Europe (Ustaszewski et al. 2010). The Drina–Ivanjica Unit is a composite nappe unit of the Internal Dinarides, which was an eastern distal part of the Adriatic microplate (Bortolotti et al. 2005; Schmid et al. 2008, 2020; Gawlick et al. 2017). The Adriatic affinity of the Drina–Ivanjica Unit might be recognized in paleomagnetic directions, since westerly declinations have been systematically observed in stable and imbricated Adria (Márton & Veljović 1983, 1987; Márton & Milićević 1994; Márton et al. 2003, 2008, 2010, 2011, 2014, 2017, 2022a; Márton & Moro 2009; Werner et al. 2015). The youngest formations which still indicate CCW rotation are of Eocene age from the stable Istria

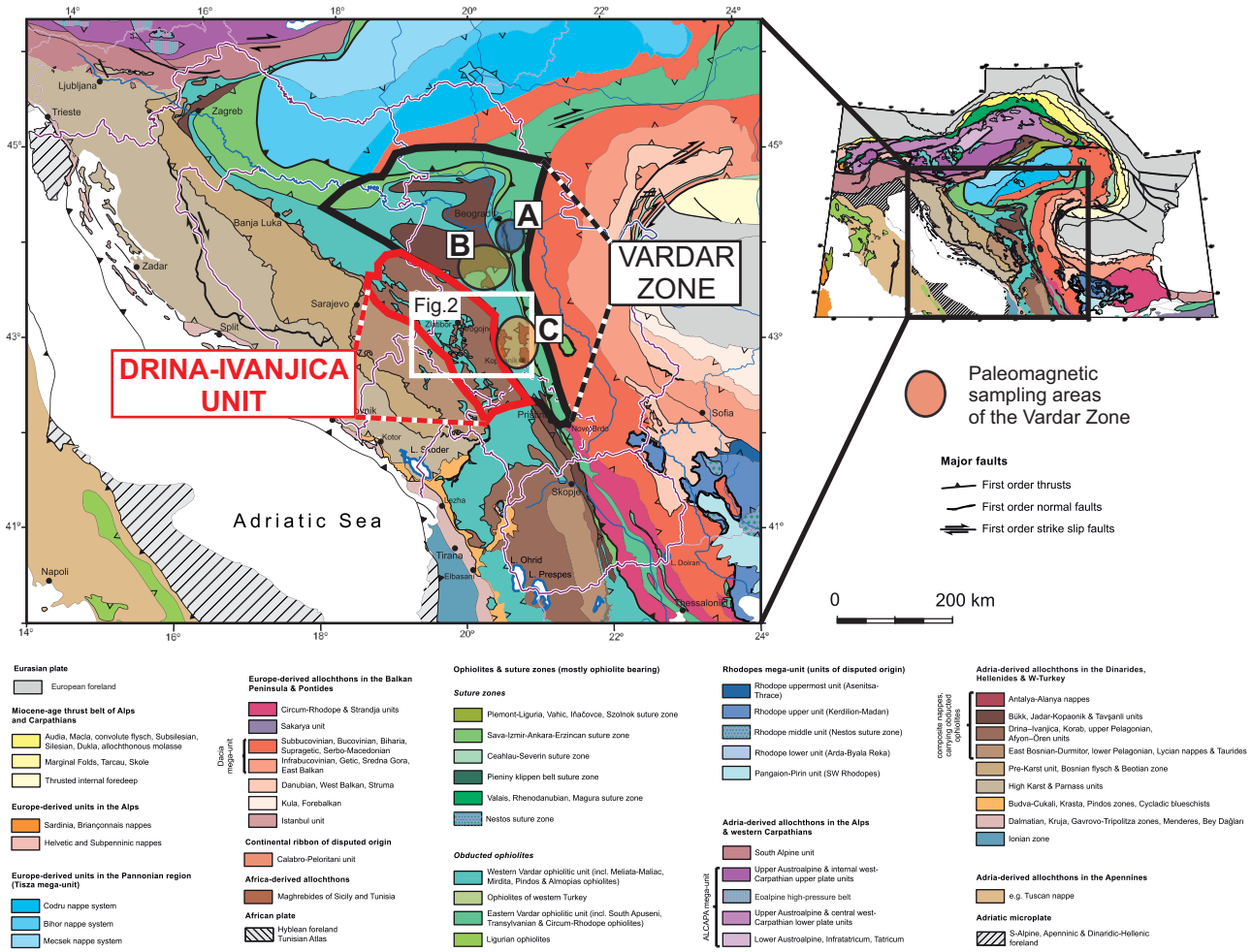

Fig. 1. Tectonic map of the Dinarides (after Schmid et al. 2020). Paleomagnetic sampling areas of earlier studies from the Vardar Zone are shown as ellipsoids: A – Belgrade area and Avala mountains (Márton et al. 2022b); B – wider Rudnik area (Lesić et al. 2019); C – Kopaonik area (Lesić et al. 2019).

(Márton et al. 2008, 2010), the Adige embayment (Márton et al. 2011), and from Brač Island (Márton et al. 2022a). Compared to the large paleomagnetic dataset available for the External Dinarides, paleomagnetic investigations of the Internal Dinarides started only recently, with results from different tectonic units (Jadar–Kopaonik thrust sheet, Sava Zone, Cretaceous overstepping sequence of the Eastern Vardar ophiolitic unit) of the Vardar Zone sensu Toljić et al. (2018) (Lesić et al. 2019; Márton et al. 2022b). Post-orogenic Oligocene igneous rocks and remagnetized post-obduction Upper Cretaceous deposits from the Western (Adriatic affinity), Central (suture zone) and Eastern (European affinity) Vardar zones have provided evidence for their coordinated about 30° CW rotation after 23 Ma, which is connected to the extension and formation of the Pannonian Basin due to rollback of the Carpathian slab. This study presents the first paleomagnetic results from post-orogenic Miocene igneous rocks and from post-obduction Upper Cretaceous sediments of the more external Drina–Ivanjica Unit to search regional extent of the CW rotations. Additionally, we present paleomagnetic results from the pre-obduction Triassic–Jurassic strata of the Drina–Ivanjica Unit, which are supposed to have originated on the distal passive margin of the Adriatic microplate (e.g., Gawlick et al. 2017), and should therefore record the well-documented CCW rotation of Adria (e.g., Márton et al. 2017 and references therein).

Geological background

The Dinarides consist of two main parts: the External and Internal Dinarides (Fig. 1). The External Dinarides are composed predominantly of Triassic to Eocene shallow water platform carbonates occasionally intercepted by zones of deep-water deposition. The Internal Dinarides are dominated by Jurassic ophiolites and continental tectonic units derived from distal passive margins of Adria (Africa-derived microplate) and Europe (Tisza and Dacia units). The nappe-system is covered by post-orogenic sedimentary formations and intruded by Oligocene to Miocene igneous rocks (e.g., Schmid

et al. 2008, 2020; Cvetković et al. 2016; Toljić et al. 2018, 2019).

The Drina–Ivanjica Unit represents one of the Adria-derived composite nappe units of the Internal Dinarides that passively carry obducted ophiolites and overstep sedimentary formations (Schmid et al. 2008, 2020), intruded by post-orogenic Miocene igneous rocks (Cvetković et al. 2004, 2016; Schefer et al. 2011). In the west, the Drina–Ivanjica Unit overthrusts the East Bosnian-Durmitor composite thrust sheet. The thrust zone has a character of out-of-sequence thrusting, cutting up obducted ophiolite massifs that had ceased by the early Late Cretaceous (Schmid et al. 2008). The observed top-to-WNW deformation formed under anchizonal metamorphic conditions and was dated by K–Ar method at 150–135 Ma (Porkoláb et al. 2019). In the east, the Drina–Ivanjica Unit is overthrust by another even more distal Adria-derived unit – the Jadar–Kopaonik Unit (Dimitrijević 1997; Schmid et al. 2008, 2020). The two units are separated by a long belt of highly deformed uppermost Cretaceous syn-contractional turbidites (the Kosovska Mitrovica Flysch of Dimitrijević 1997). The contact zone is affected by a Late Cretaceous–Paleocene dextral transpressive fault system (Zvornik Fault/suture; Karamata et al. 1994; Dimitrijević 1997). The nappe-pile east of the Drina–Ivanjica Unit is also denoted as the Vardar Zone (e.g., Kossmat 1924; Dimitrijević 1997; Cvetković et al. 2016; Toljić et al. 2018, 2019), which is a 40–70 km wide zone, comprising units that derive from the Adriatic passive margin, the oceanic lithosphere of the Meliata, Vardar, and Sava oceans, or the distal European margin (Cvetković et al. 2016). It is divided into three subzones (Toljić et al. 2019): The Western Vardar Zone of Adriatic affinity (also known as Srem, Jadar, and the Kopaonik blocks or Jadar–Kopaonik thrust sheet; e.g., Dimitrijević 1997; Schmid et al. 2008), the Eastern Vardar Zone of European affinity (the Eastern Vardar ophiolitic unit obducted over the Serbo–Macedonian massif), and the Central Vardar Zone representing the suture between the two (the Sava Zone of Schmid et al. 2008, 2020).

The Drina–Ivanjica Unit is composed of a Late Paleozoic low-grade metamorphic basement (Milovanović 1984; Trivić et al. 2010) overlain by Triassic–Jurassic sedimentary cover deposited on the distal continental margin of the Adriatic microplate (Gawlick et al. 2017). The oldest Triassic strata are represented by continental siliciclastic rocks that grade into a mixed siliciclastic–carbonate marine succession (Dimitrijević 1997). The Middle Triassic is represented by Anisian Gutenstein- and Steinalm-type limestones followed by the deposition of Ladinian–Carnian, thin-bedded, red nodular and siliceous limestones (Sudar 1986; Dimitrijević 1997; Chiari et al. 2011). Substantial deepening of the Adriatic margin prior to ophiolite obduction is manifested by the deposition of cherty limestones and radiolarites during the Early and Middle Jurassic (Djerić et al. 2007; Gawlick et al. 2009, 2016; Chiari et al. 2011). The basement-cover of the Drina–Ivanjica Unit occurs as tectonic windows from below obducted ophiolite, with tectono-sedimentary mélange at its base. Ophiolites of the Drina–Ivanjica Unit consist of serpentinized peridotites, harzburgites, gabbros, diabases, basalts, and locally, granites (Dimitrijević 1997; Pamić et al. 2002; Chiari et al. 2011). The obduction of ophiolites onto the Drina–Ivanjica Unit took place during the Late Jurassic to Early Cretaceous times (Dimo-Lahitte et al. 2001; Borojević-Šoštarić et al. 2012, 2014; Gawlick et al. 2016, 2017).

The ophiolites and underlying Drina–Ivanjica basement-cover are truncated by an erosional unconformity and sealed by sedimentation of clastic terrestrial deposits rapidly followed by a widespread carbonate platform system since the late Early Cretaceous (Chiari et al. 2011; Nirta et al. 2020). At present, the Cretaceous sediments crop out over areas of varying extension – from hundred-kilometre-wide, undeformed, continuous cover units to small-scale, tectonically-disintegrated slivers (Nirta et al. 2020). The overstep deposits consist of terrestrial, transitional, and shallow-marine coarse-grained clastic sedimentary rocks and of marine fine-grained clastic sediments and carbonates passing to flysch-type rocks. In the studied area, the overstep deposits are divided into three lithostratigraphic groups according to their age and depositional environment (Chiari et al. 2011; Nirta et al. 2020). The Mokra Gora Group sediments (upper Aptian–Maastrichtian) were deposited on top of previously-obducted and eroded ophiolites; the Kosjerić Group (Cenomanian–Campanian) overlies both ocean-derived and continental-derived rocks, while the Guča Group (Campanian–Maastrichtian) covers the continental basement exclusively (Nirta et al. 2020). The Mokra Gora succession starts with discontinuous beds of laterites, which are covered by sandstones and marls bearing ophiolitic detritus (Nirta et al. 2020). These are topped by Albian to Cenomanian (Banjac 1994) reddish, fossiliferous limestones and marlstones (Nirta et al. 2020). The Mokra Gora Sequence is terminated by massive, thick-bedded rudist bearing limestones of middle Turonian–Santonian age (Radoičić & Schlagintweit 2007). The Kosjerić Group is made up of upper Cenomanian shallow marine limestones that gradually pass into middle Turonian–lower Campanian hemipelagic marlstones (Radoičić & Schlagintweit 2007). The Guča Group succession starts with littoral to slope facies clastic deposits, followed by well-bedded limestones and calcareous sandstones, which develop upwards into rudist-bearing massive limestones (Chiari et al. 2011; Nirta et al. 2020). The uppermost part is made of Campanian to Maastrichtian (Danian?) turbidite beds composed of calcareous marls, graded biosparites, siltstones, and olistostromes (Ćirić 1958; Dimitrijević 1997; Dimitrijević & Dimitrijević 2009).

The final closure of the Neotethys (Vardar) Ocean and the subsequent continental collision was, after the Late Eocene, followed by a transtensional tectonic regime associated with core-complex exhumation and the opening of small sedimentary basins (Ilić & Neubauer 2005; Ustaszewski et al. 2010; Zelic et al. 2010). The extension also triggered Miocene magmatic activity, which is represented in the studied area by the Golija pluton and by small ultrapotassic basalt flows with associated volcanoclastics (Fig. 2). The Golija pluton consists of high-K calc-alkaline, I-type granodiorite intrusions and

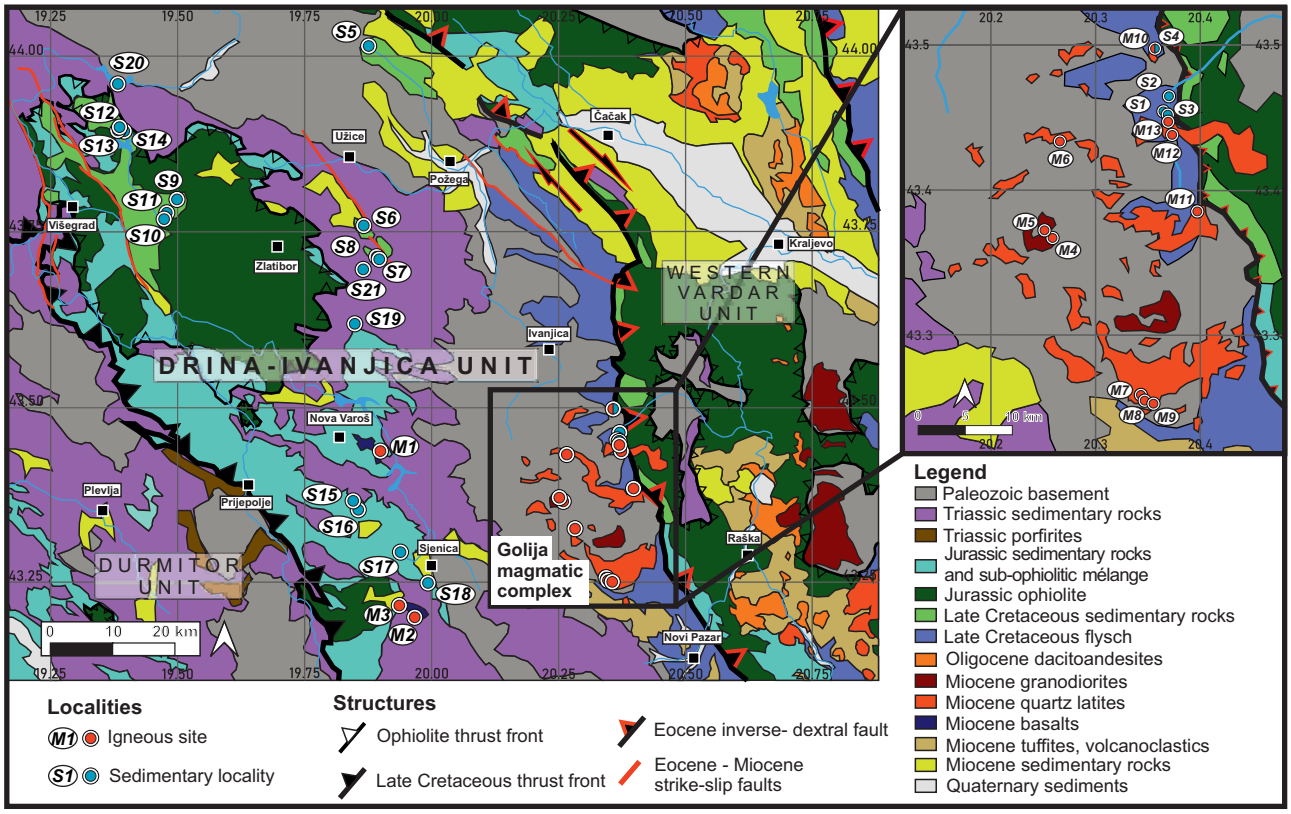

Fig. 2. Simplified geological map (WGS 84, Pseudo-Mercator projection, EPSG:3857) of the central part of the Drina–Ivanjica Unit, based on 1:100 000 sheets of Geological Maps of former Yugoslavia (Osnovna Geološka Karta SFRJ). Paleomagnetic sampling localities/sites are shown as dots.

quartz latite extrusions and volcanoclastics with ages determined by U–Pb dating of zircons at 20.58–20.17 Ma (Schefer et al. 2011). Intrusive rocks of the Golija pluton are compositionally-similar to the granitoids of the Kopaonik and Drenje massifs (belonging to the Western Vardar Zone of Toljić et al. 2019), but contain more potassium and show higher crustal influence during their magma generation (Schefer et al. 2011).

Paleomagnetic sampling and laboratory processing

Paleomagnetic samples were drilled with a portable gasoline-powered or cordless electrical drill with water cooling. Orientation of the samples was done with a magnetic compass, or in the case of magmatic rocks, with a sun compass as well. Altogether, 358 individually-oriented samples were drilled at 34 sites/localities covering a variety of rocks representing different ages, lithology, and depositional settings (Fig. 2, Tables 1, 2, 3). Basalts (K–Ar age 9.1, 21.5 and 23.0 Ma, Cvetković et al. 2004) outcropped east of Nova Varoš and southwest of Sjenica were sampled at three sites (sites M1–M3). In the Miocene Golija pluton (inset in Fig. 2, Table 2), ten sites were sampled (M4–M13) from granodiorites (U–Pb age 20.6–20.2 Ma, Schefer et al. 2011) and quartz latites. In the Golija area, we also sampled overstep Campanian–Maastrichtian dark grey flysch deposits of the Guča Group (Table 3, localities S1–S4; Chiari et al. 2011), including one from the thermocontact zone of quartz latite (locality S4).

Overstep late Early to Late Cretaceous clastic-carbonate deposits, preserved either on top of the obducted ophiolites or directly on the basement/cover of the Drina–Ivanjica Unit, were sampled at geographically-distributed localities (Fig. 2, Table 3). From the Kosjerić Group (Chiari et al. 2011; Nirta et al. 2020), outcropped in the north-eastern part of the study area, Turonian–Campanian marls were sampled (Fig. 2, Table 3, locality S5). From the occurrences of the Late Cretaceous deposits east of the Zlatibor massif, we sampled Cenomanian–Turonian marly dolomitic limestones underlain with bauxite mudcakes (localities S6–S8). West of the Zlatibor massif, Cenomanian–Turonian pelagic carbonates of the Mokra Gora Group (Chiari et al. 2011; Nirta et al. 2020) were sampled (Fig. 2, Table 3, localities S9–S14).

The sampled Triassic–Jurassic cover strata of the Drina–Ivanjica Unit included thin-bedded to massive Lower to Middle Jurassic limestones (localities S15–S18) outcropped near Sjenica. Upper Triassic thin-bedded limestones (localities S19, S20) and Anisian Rosso Ammonitico limestones (locality S21) were sampled in the area north-west and east of the Zlatibor massif (Fig. 2, Table 3).

Table 1: Summary of site/locality mean Anisotropy of Magnetic Susceptibility (AMS) directions. AMS was measured on those rocks which have susceptibility of at least 10^{-4} SI. Key: n – number of specimens (standard analysis: multiple specimens from one sample); κ – mean susceptibility; D, I, conf – declination, inclination and the related confidence ellipse of the maximum, intermediate and minimum directions (upper row before; lower row after tilt correction); mean L, F – degree of lineation, foliation; mean P – mean of the degree of anisotropy; average P – average degree of anisotropy for the site/locality. The results were evaluated using Anisoft 4.2 (Chadima & Jelínek 2008) based on Jelínek & Kropáček (1978). The sites/localities are numbered according to Fig. 2.

Code	Locality	Lat. N [°] Lon. E [°]	n	κ 10^{-6} SI	max D° D_c°	max I° I_c°	max conf	inter D° D_c°	inter I° I_c°	inter conf	min D° D_c°	min I° I_c°	min conf	Mean L (%)	Mean F (%)	Mean P (%)	Average P (%)
Miocene basalts																	
M1	Podomar YM 3250-255	43.4380 19.8992	6	20600	247.0	32.6	18.6/ 13.7	149.8	11.0	22.2/ 16.2	43.6	55.1	24.9/ 11.3	1.6	0.9	2.5	2.9
M3	Trijebine YM 3265-268	43.2169 19.9364	6	16800	357.8	2.0	9.5/ 5.9	87.8	2.2	9.2/ 4.3	225.5	87.0	6.9/ 4.9	0.2	0.2	0.5	0.5
Golija magmatic complex																	
Miocene granodiorites																	
M4	Golijska Reka 1 Z 73-78	43.3661 20.2591	11	343	265.2	23.7	38.8/ 30.6	173.5	3.7	54.4/ 36.8	75.1	66.0	54.0/ 29.1	6.4	4.2	10.9	23.9
M5	Golijska Reka 2 Z 127-131	43.3714 20.2514	9	454	92.7	0.7	30.3/ 11.3	2.5	17.1	30.3/ 14.9	184.9	72.9	19.2/ 11.1	4.2	7.6	12.1	17.4
Miocene quartz latites																	
M6	Pakašnica Z 65-72	43.4331 20.2661	9	7290	216.3	61.6	52.3/ 11.6	114.8	6.1	52.3/ 20.8	21.6	27.6	21.3/ 11.5	0.2	1.2	1.5	2.1
M7	Odvraćenica 1 Z 137-145	43.2569 20.3436	26	6580	66.0	11.1	45.0/ 27.2	164.4	36.6	44..6/ 26.9	321.9	51.2	32.9/ 20.5	0.3	0.9	1.1	1.8
M8	Odvraćenica 2 Z 146-152	43.2529 20.3472	13	13800	358.0	40.8	33.8/ 9.1	244.5	24.8	35.3/ 16.2	132.5	39.1	20.3/ 9.2	0.8	1.5	2.3	3.1
M9	Odvraćenica 3 Z 153-158	43.2508 20.3556	10	16500	235.0	27.2	8.9/ 4.5	342.4	30.1	8.3/ 4.4	111.3	47.3	6.3/ 3.6	0.6	1.5	2.1	2.2
M10	Veljovići Z 173-178	43.4983 20.3576	6	207	138.4	55.4	11.8/ 4.6	351.0	30.2	13.6/ 5.1	251.9	15.3	9.3/ 4.6	0.4	0.5	0.8	0.9
M11	Devići 1 Z 189-195	43.3845 20.3975	7	189	176.2	83.7	51.3/ 6.7	345.0	6.2	51.3/ 8.1	75.1	1.2	9.1/ 6.8	0.1	0.7	0.9	1.0
M12	Devići 2 Z 196-201. 278-283	43.4377 20.3735	16	6250	224.2	8.9	24.1/ 10.6	358.8	77.5	24.6 14.5	132.8	8.8	16.1 9.6	0.5	1.5	2.0	2.6
M13	Devići 3 Z 266-277	43.4468 20.3697	21	10700	98.0	1.6	10.5/ 5.5	189.1	34.2	8.3 4.5	5.6	55.8	10.1 7.0	0.9	1.6	2.5	2.8
Upper Cretaceous flysch																	
S1	Studenica valley 1 Z 159-172	43.4540 20.3651	14	377	92.5 98.6	31.6 1.2	7.3/2.6 7.6/2.7	188.9 8.5	10.3 5.8	6.3/5.0 7.2/3.1	294.8 200.1	56.3 84.1	5.3/4.5 4.6/3.3	1.5	6.5	8.1	8.2
S2	Studenica valley 2 Z 202-211	43.4645 20.3704	10	383	75.0 248.3	30.8 5.9	12.7/ 1.9	202.1 109.4	45.3 82.2	12.8/ 8.1	325.9 338.8	28.8 5.1	8.2/ 1.6	2.0	4.5	6.6	6.8
S3	Studenica valley 3 Z 284-292	43.4517 20.3693	14	359	116.6 123.5	36.9 5.1	5.8/ 4.1	221.9 214.0	19.5 6.1	11.9/ 5.6	333.9 354.1	46.7 82.0	11.9/ 4.0	2.9	3.0	6.0	6.5
S4	Veljovići Z 179-188	43.4983 20.3576	10	433	131.5 111.1	73.1 7.0	5.9/ 4.5	20.0 201.5	6.4 4.0	8.4/ 4.3	288.2 321.3	15.6 81.9	8.2/ 5.9	2.0	3.6	5.7	5.9
Middle Jurassic limestones																	
S15	Suvi Bor 1 Z319-326	43.3541 19.8556	10	121	8.5 7.8	3.3 17.8	12.1/ 8.6	100.0 107.0	24.0 26.5	25.0/ 8.2	271.2 247.9	65.7 57.2	23.7/ 8.6	0.7	0.7	1.5	1.7
S16	Suvi Bor 2 Z327-339	43.3668 19.8455	14	122	319.2 312.3	19.5 14.1	16.5/ 5.5	224.0 44.3	14.2 8.0	20.4/ 7.9	100.2 163.1	65.5 73.7	15.0/ 6.4	0.8	0.8	1.6	1.7

From the drilled cores, one or several standard-size, one-inch diameter specimens were cut in the laboratory. The NRM (Natural Remanent Magnetization) was mesured using a JR-4 and JR-5 spinner magnetometers (Agico, Brno, former Geofyzika Brno). Afterwards, anisotropy of magnetic susceptibility (AMS) using a KLY-2 Kappabridge (Agico, Brno, former Geofyzika Brno) was measured. The AMS measurements were carried out on rocks with susceptibilities in order of at least 10^{-4} SI. The AMS data were evaluated on sample level with the Aniso program (Bordás 1990) and at site/locality level by Anisoft 4.2 software (Chadima & Jelínek 2008), both based on the research of Jelínek & Kropáček (1978).

For pilot specimens from each sampled group, stepwise thermal (TH) and alternating field (AF) demagnetizations were carried out. For thermal demagnetization, a TSD-1 thermal demagnetizer (Schonstedt Instrument Company, Reston) was used. Magnetic susceptibility was measured after each heating step to detect changes in magnetic mineralogy during thermal demagnetization. Alternating field demagnetization was carried out on LDA-3A (Agico, Brno) and Demag 01-79 (Technical University, Budapest) demagnetizers. Based on the behaviour of the pilot samples during demagnetization, the remaining samples were demagnetized by the more efficient method and in as many steps as was necessary to isolate a ChRM (Characteristic Remanent Magnetization) component. The components of the NRM were determined by principal component analysis (Kirschvink 1980). Mean paleomagnetic directions for each locality/site were calculated using Fisher (1953) statistics. Paleomagnetic stability tests (e.g., tilt test, reversal test) were made with PMGSC 4.2 (Enkin 2003a) and PMagTools 4.2 (Hounslow 2006) software. To identify magnetic minerals magnetic mineralogy experiments were carried out on selected specimens. These experiments included acquisition of laboratory-induced remanent magnetization (IRM) using a Molspin pulse magnetizer (maximum field 1 T), followed by a thermal demagnetization of the three-component IRM (Lowrie 1990) accompanied by susceptibility monitoring; and thermal vs. susceptibility measurements up to 700 °C, either from liquid nitrogen temperature or from room temperature using a KLY-2 Kappabridge combined with CSL Low Temperature Cryostat and CS-3 High Temperature Furnace apparatuses (AGICO, Brno; Parma et al. 1993; Hrouda 1994). All laboratory experiments were carried out in the Paleomagnetic Laboratory at SARA, Budapest (former Mining and Geological Survey of Hungary).

Table 2: Summary of site mean paleomagnetic directions of the Miocene igneous sites from the Drina–Ivanjica Unit. K–Ar ages for the basalts are 21.5 Ma (M1) and 23.0 Ma (M3) from Cvetković et al. (2004), U–Pb age for the granodiorites is 20.6–20.2 Ma from Schefer et al. (2011). Estimated ages for the quartz latites are the same as for the granodiorites. Key: Lat. N and Lon. E – geographic coordinates (WGS 84), n/no – number of used/collected samples; D, I – declination, inclination (corrected declination with IGRF-13 model, Alken et al. 2021); k and α95 – statistical parameters (Fisher 1953). Sites are numbered according to Fig. 2. * Mean direction was evaluated with great circle analysis combined with stable point, defined as the overall mean direction of the remaining sites (McFadden & McElhinney 1988). ** Mean direction was calculated from stable end points.

Code	Locality	Lat. N [°] Lon. E [°]	n/no	D [°]	I [°]	k	a95 [°]
Basalts							
M1	Podomar * YM 3250-255	43.4380 19.8992	5/6	190.8	−55.5	–	–
M3	Trijebine YM 3265-268	43.2169 19.9364	13/13	195.5	−59.2	242.0	2.7
Golija magmatic complex							
Granodiorites							
M4	Golijska Reka 1 * Z 73-78	43.3661 20.2591	5/6	205.1	−57.0	–	–
M5	Golijska Reka 2 Z 127-131	43.3714 20.2514	0/5	large scatter			
Quartz latites							
M6	Pakašnica Z 65-72	43.4331 20.2661	0/8	large scatter			
M7	Odvraćenica 1 Z 137-145	43.2569 20.3436	9/9	220.7	−41.8	285.0	3.1
M8	Odvraćenica 2 Z 146-152	43.2529 20.3472	6/7	220.8	−37.0	195.0	4.8
M9	Odvraćenica 3 * Z 153-158	43.2508 20.3556	6/6	178.8	−50.6	–	–
M10	Veljovići Z 173-178	43.4983 20.3576	0/6	large scatter			
M11	Devići 1 ** Z 189-195	43.3845 20.3975	6/7	227.3	−74.4	35.9	11.3
M12	Devići 2 Z 196-201, 278-283	43.4377 20.3735	8/12	45.2	+63.9	27.7	10.7
M13	Devići 3 Z 266-277	43.4468 20.3697	10/12	333.9	+41.0	98.0	4.9

Results

Miocene magmatic rocks

Quartz latites of the Golija pluton show highly-varying susceptibilities (10^{-2}–10^{-4} SI) and are characterized by weak anisotropy. The low degree of anisotropy was also observed in basalts. The magnetic foliation is well-developed in the quartz latites, while in the basalts, it is weak (Table 1). Granodiorite samples have high AMS (P_{max}=45 %), but the AMS ellipsoids are not well-clustered at the site level (Table 1).

The IRM acquisition curves indicate that the dominant magnetic carrier in the quartz latites is a soft coercivity magnetic

Table 3: Summary of locality mean paleomagnetic directions of the sedimentary localities from the Drina–Ivanjica Unit. Localities S4, S5, S9 and S15 did not give results due to the large scatter. Key: Lat. N and Lon. E – geographic coordinates (WGS84), n/no – number of used/collected samples; D, I – declination, inclination (corrected declination with IGRF-13 model, Alken et al. 2021); k and α95 – statistical parameters (Fisher 1953) Dc, Ic – declination, inclination after tilt-correction. The localities are numbered according to Fig. 2. **Bold**: data used for overall mean direction calculation. * Mean direction was evaluated with stable end points. ** Mean direction was evaluated with stable end points and great circle analysis (McFadden & McElhinney 1988).

Code	Locality	Age	Lithology	Lat.N [°] Lon.E [°]	n/no	D [°]	I [°]	k	a95 [°]	Dc [°]	Ic [°]	k	a95 [°]	dip
Upper Cretaceous														
Golija area														
S1	Studenica valley 1 Z 159-172	Campanian–Maastrichtian	dark grey flysch	43.4540 20.3651	9/14	**37.0**	**+56.3**	**93.1**	**5.4**	84.3	+47.1	72.9	6.1	variable
S2	Studenica valley 2 Z 202-211	Campanian–Maastrichtian	dark grey flysch	43.4645 20.3704	9/10	**1.9**	**+62.4**	**46.8**	**7.6**	21.1	+20.3	46.8	7.6	38/46
S3	Studenica valley 3 Z 284-292	Campanian–Maastrichtian	dark grey flysch	43.4517 20.3693	4/9	**61.9**	**+56.8**	**59.9**	**12.0**	105.1	+43.6	59.9	12.0	154/36
Zlatibor area														
S6a	Skržuti, *upper beds* Z 212-223, 293-318	Cenomanian–Turonian	dolomitic limestone	43.7596 19.8663	19/24	8.3	+50.3	62.6	4.3	**25.5**	**43.9**	**62.6**	**4.3**	85/17
S6b	Skržuti, *lower beds* Z 293-318	Cenomanian–Turonian	marly dolomitic limestone	43.7596 19.8663	11/14	12.0	+47.7	177.0	3.4	**27.1**	**+40.5**	**177.0**	**3.4**	85/17
S7	Ravni 1 Z 340-349	Cenomanian–Turonian	dolomitic limestone	43.7129 19.8942	8/10	21.2	+64.9	74.7	6.5	**30.7**	**+39.8**	74.7	6.5	42/26
S8	Ravni 2 * Z 350-357	Cenomanian–Turonian	dolomitic limestone	43.7116 19.8968	8/8	17.5	+63.7	74.7	6.5	**27.6**	**+59.3**	74.7	6.5	74/7
Mokra Gora area														
S10	Mokra Gora 2 Z 113-119	Cenomanian–lower Turonian	pelagic limestone	43.7687 19.4733	6/7	95.4	+63.5	77.6	7.7	**16.1**	**+51.5**	**77.6**	**7.7**	337/45
S11	Mokra Gora 3 Z 120-127	Cenomanian–lower Turonian	pelagic limestone	43.7777 19.4786	7/8	32.7	78.3	298.7	3.5	**342.9**	**+54.2**	**298.7**	**3.5**	324/30
S12	Zaovine lake 1 Z 1-10	Cenomanian–lower Turonian	pelagic limestone	43.8993 19.3856	7/10	310.1	+67.9	66.4	7.5	**358.4**	**+38.0**	**66.4**	**7.5**	26/43
S13	Zaovine lake 2 Z 11-24	Cenomanian–lower Turonian	pelagic limestone	43.8971 19.3846	13/14	6.7	+61.6	72.5	4.9	**6.4**	**+34.6**	**72.5**	**4.9**	6/27
S14	Zaovine lake 3 Z 224-232	Cenomanian–lower Turonian	pelagic limestone	43.8937 19.3948	8/9	34.1	+50.3	41.8	8.7	**21.5**	**+63.0**	**41.8**	**8.7**	241/15
Jurassic														
S16	Suvi Bor 2 ** Z 327-339	Middle Jurassic	red limestone	43.3668 19.8455	7/13	**330.5**	**+50.1**	**58.6**	**8.2**	306.3	+43.7	58.6	8.2	244/23
S17	Krš Gradac Z 91-104	Lower Jurassic–Bajocian	red limestone	43.2934 19.9387	13/14	**333.6**	**+58.2**	**29.9**	**7.7**	278.9	+48.2	28.0	8.0	variable
S18	Sjenica Z 79-90	Lower Jurassic	thin-bedded to massive limestone	43.2492 19.9928	9/12	36.9	+41.8	37.6	8.5	**322.1**	**+60.0**	**37.6**	**8.5**	255/54
Triassic														
S19	Ljubiš Z 53-64	Upper Triassic	thin-bedded limestone	43.6197 19.8487	9/12	38.9	+49.5	12.8	15.0	26.2	+22.1	15.9	13.3	variable
S20	Perućac lake Z 25-33	Anisian	thin-bedded limestone	43.9606 19.3823	9/9	**351.7**	**+46.1**	**44.1**	**7.8**	299.8	+65.8	44.1	7.8	208/37
S21	Klisura quarry Z 34-52	Anisian	rosso ammonitico	43.6972 19.8653	19/19	**353.0**	**+56.9**	**75.7**	**3.9**	314.8	+37.4	75.7	3.9	272/38

mineral (Fig. 3). Susceptibility vs. temperature experiments proved that this soft, magnetic mineral is magnetite (Verwey-transition at ≈−150 °C, susceptibility falls near 580 °C, reversible cooling and heating curves; Fig. 3, M9, M12). The sample from site M7, representing one block only, shows a different magnetic behaviour, as the saturation was slower during the IRM acquisition, and the susceptibility frequently changed during heating (Fig. 3, M7). The susceptibility changes are probably connected to the exsolution of titanomagnetite into magnetite and paramagnetic ilmenite (Curie-point at 580 °C, smooth cooling curve). Changes in magnetic mineralogy were obvious during thermal demagnetization as well (susceptibility changes; Fig. 4, M7a). In granodiorites, paramagnetic minerals are dominant (Fig. 3, M4).

For the majority of sites, stepwise TH or AF demagnetizations provided excellent linear segment decaying towards the origin of the Zijderveld diagram (Zijderveld 1967; e.g., Fig. 4, M3, M7a, M7b). These segments were defined by the demagnetizing steps between 400–580 °C (TH) or between 20–100 mT (AF). Composite NRMs were characteristic for some of the igneous sites, where the paleomagnetic vector during demagnetization moved along the remagnetization circle (Fig. 5). In such cases, the overprint magnetization was either eliminated (by 15 mT; Fig. 4, M12) or a portion of it resisted the demagnetization, resulting in a shallow inclination (Fig. 5, M1, M4 and M9). In the latter cases, great circle analysis combined with stable end-points (McFadden & McElhinney 1988), the latter, defined as the well-clustered site mean directions of the remaining sites, provided useful site means for further interpretation (Table 2). Site M2 was excluded from the tectonic interpretation due to the significantly younger age (9.1 Ma; Cvetković et al. 2004).

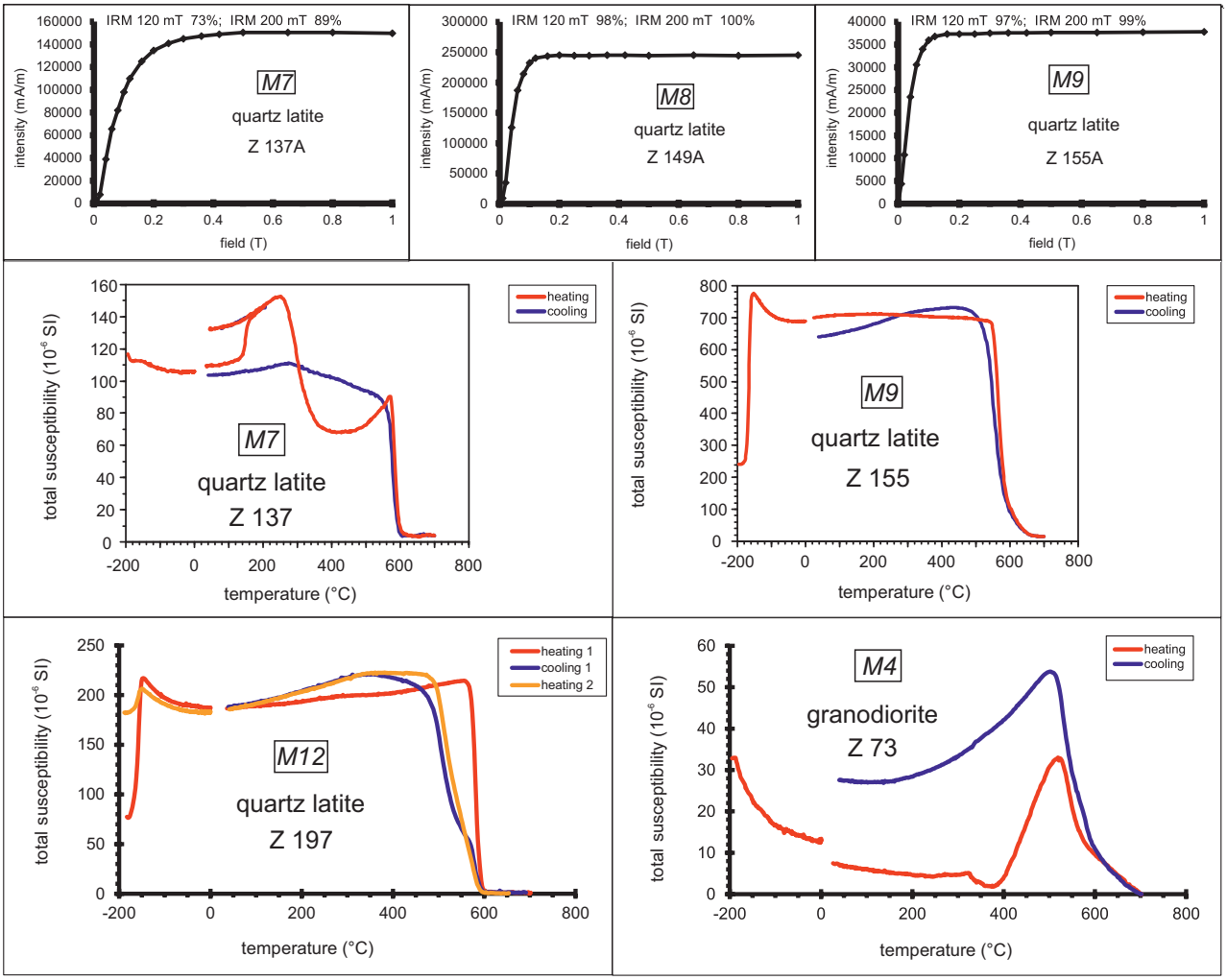

Fig. 3. Magnetic mineralogy experiments of the Miocene magmatic rocks, Golija area. First row: typical IRM acquisition curves; second and third rows: typical magnetic susceptibility vs. temperature curves. Magnetite can be identified in quartz latites (quick IRM saturation, low-temperature Verwey-transition, susceptibility drop near 580°, identical cooling and heating curves), except for one block of site M7 (slower saturation, susceptibility changes between 150–400 °C). Granodiorite samples (M4) have substantial amount of paramagnetic minerals (highly visible paramagnetic hyperbola during heating).

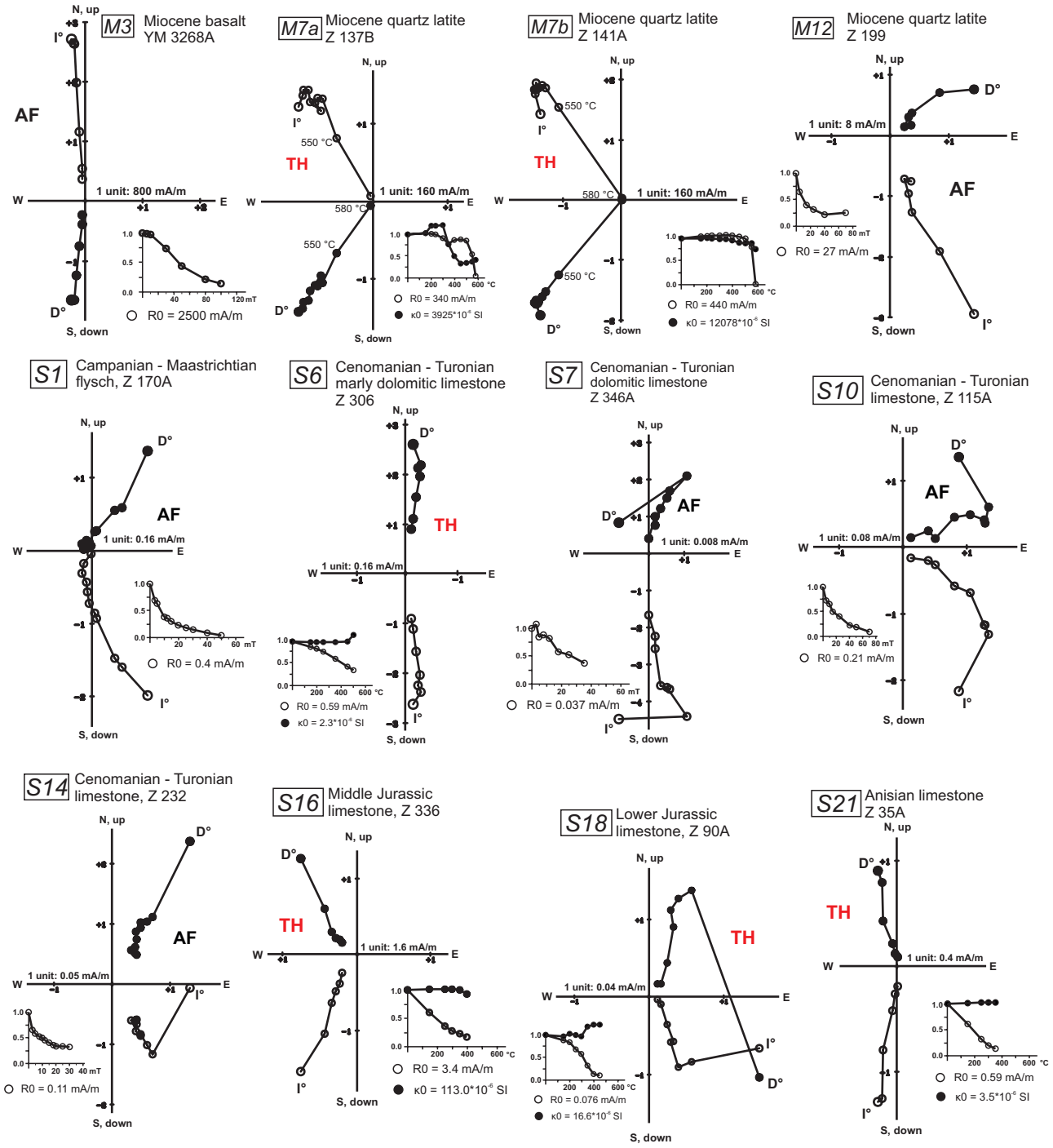

Fig. 4. Typical demagnetization curves for igneous and sedimentary rocks of the Drina–Ivanjica Unit. Some of the quartz latites (e.g., M12) and limestones (e.g., S10, S18) have composite NRMs. Samples from the block of *M7a* and locality *S18* indicate mineralogical changes during TH demagnetization. Key: Zijderveld diagrams (Zijderveld 1967) are oriented in geographically and, in the case of **AF** demagnetization they are accompanied by intensity (open circles) vs. demagnetizing field diagrams and by NRM intensity (open circles)/susceptibility (full circles) vs. temperature diagrams, when the method is thermal (**TH**) demagnetization. In the Zijderveld diagrams, full dots are the projections of the NRM vector onto the horizontal; circles – into the vertical. Site/locality numbers are identical with Tables 2, 3 and Fig. 2.

Campanian–Maastrichtian flysch – Golija area

Magnetic susceptibility values are consistent for flysch-type rocks of the Golija area and are in the range of 10^{-4} SI. The magnetic fabric is characterized by a dominant foliation with sub-ordinate lineation (Table 1). The magnetic fabric is most likely governed by a mixture of paramagnetic and ferromagnetic minerals. The former can be pyrite, indicated by

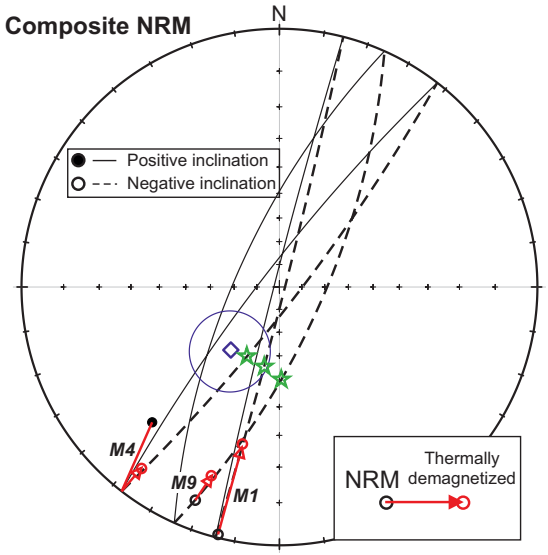

Fig. 5. Typical behaviour of the composite NRMs of the Miocene magmatic samples during demagnetization (the directions move along the remagnetization curves). Plotted sites had overprint magnetization, which could not be eliminated by the demagnetization procedures. Overall mean direction was calculated (blue square) for the well-clustered remaining sites (M3, M7, M8, M11, M12). Combined great circle analysis (McFadden & McElhinney 1988) with stable end point (overall mean direction) resulted in new paleomagnetic directions (green stars) for the sites M1, M4 and M9.

Fig. 6. IRM acquisition curves and thermal demagnetization of the three component IRM (method by Lowrie 1990) in sedimentary rocks from the Drina–Ivanjica Unit. Presence of high coercivity magnetic mineral (goethite or hematite) was recognised at localities S6, S16, S18 and S21. The soft components decay by the Curie-point of magnetite. From top to bottom: IRM acquisition; thermal demagnetization of the three-component IRM; susceptibility after each heating step. The components of the IRM were acquired in fields of 1.0 T (squares), 0.36 T (full circles) and 0.12 T (open circles).

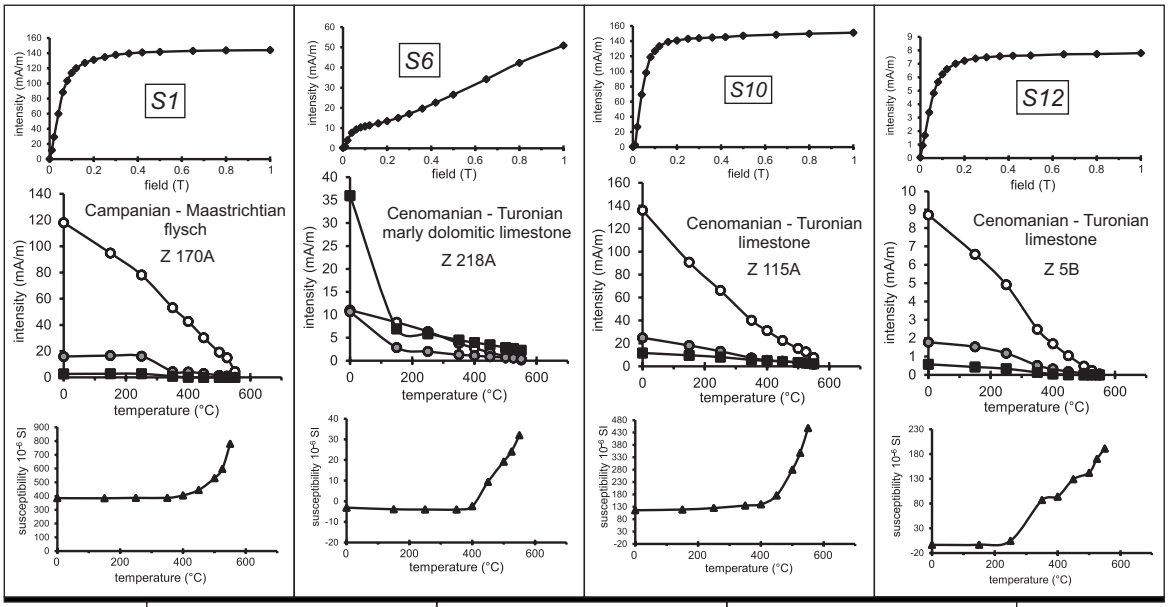

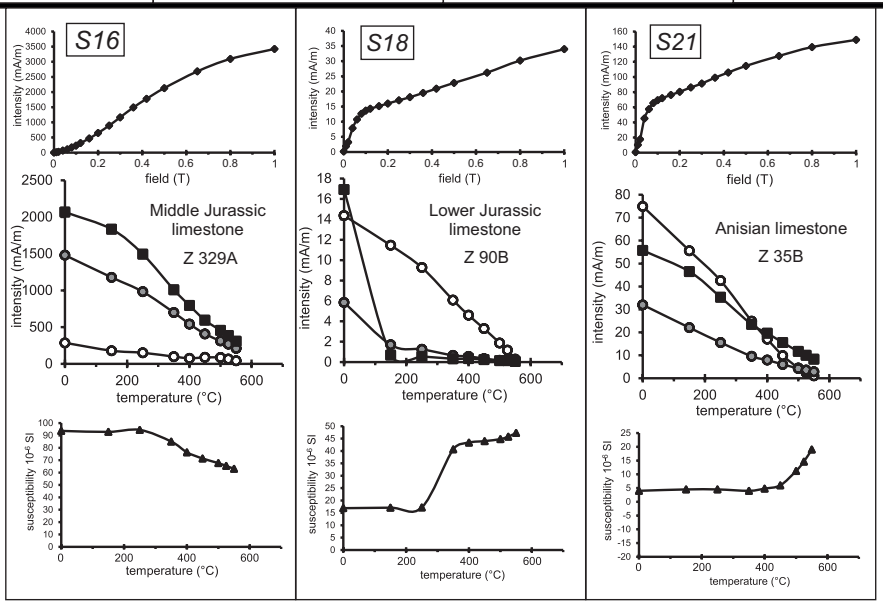

susceptibility growth after 400 °C (Fig. 6, S1); the latter can be magnetite (Fig. 6, S1).

The AF demagnetizations resulted in linear components and did not decay to the origin of the Zijderveld diagram (Fig. 4, S1). Most of the flysch samples were destroyed by heating above 350–400 °C during thermal demagnetization. The linear segments in both cases had similar directions; therefore, it was possible to define the direction of an overprint component between 5–20 mT or 150–350 °C (Table 3). In some samples, the presence of a more stable magnetization was detected at 400–500 °C (the paleomagnetic direction moved along the remagnetization circle, Fig. 4, S1), but the attempt to determine the direction of that component failed, as the method of intersection of remagnetization curves (Halls 1978) yielded a poorly-constrained direction.

Cenomanian–Turonian dolomitic limestones, marls – Zlatibor area

The demagnetization of the three component IRM (Lowrie 1990) indicate the presence of goethite (intensity of the hard component decreased by 150 °C, Fig. 6, S6). However, the main carrier of the NRM is magnetite based on the demagnetization experiments (no significant intensity decrease by 150 °C, intensity decayed continuously up to 580 °, Fig. 4, S6). The AF method (e.g., Fig. 4, S7) was applied to the groups that a had weak magnetic signal (10^{-2} mA/m, S6a, S7, S8), while the thermal method (e.g., Fig. 4, S6) was used for the stronger samples (S6b). Both methods resulted in statistically, well-defined mean directions (Table 3).

Cenomanian–Turonian pelagic limestones – Mokra Gora area

The IRM acquisition curves indicate that soft coercivity magnetic mineral is dominant. Based on the Lowrie experiments, it can be interpreted as magnetite (soft component decays up to 580 °C, Fig. 6, S10, S12).

The AF demagnetization method was very efficient in this group. Although the NRM was composite, the soft component was easily removed after first demagnetization steps (in alternating fields of 3–5 mT). Well-defined ChRM components were isolated at five of six localities sampled in this area (e.g., Fig. 4, S10, S14).

Triassic and Jurassic limestones

Negative susceptibilities were observed in most of the Triassic and Jurassic limestones, except for the thin-bedded Middle Jurassic red limestones sampled at localities S15 and S16, where weak anisotropy with equally-developed foliation and lineation were observed (Table 1).

The Lowrie experiments indicated the presence of a high coercivity magnetic mineral. In some cases, it is recognized as goethite. The IRM intensity dropped at 150 °C and susceptibility increased near 350 °C, suggesting the alteration of goethite to hematite (e.g., Fig. 6, S18). At other localities, the hard magnetic mineral is probably hematite, since the hard component was still significant after 550 °C (Fig. 6, S16, S21). The three component IRM demagnetization curves also revealed a soft component with the Curie-point of the magnetite. However, during the thermal demagnetization of the NRM, much of the intensity was lost by 400 °C (Fig. 4, S16, S18, S21). This can be attributed to the different grain sizes of the magnetite dominant in the NRM and the IRM respectively.

The Triassic and Jurassic limestones were predominantly thermally demagnetized (Fig. 4, S16, S18, S21), as the AF method often yielded chaotic demagnetization curves. After the elimination of the overprint component (by 250 °C), the thermal steps between 250–400 °C resulted in clear linear segments for ChRM evaluation.

Discussion

The late Oligocene–Miocene extension and volcanism produced several magmatic provinces within the Internal Dinarides and the Vardar Zone. The Early Miocene magmatism is probably connected to the rollback effect of the Carpathian subduction (e.g., Cvetković et al. 2004; Ustaszewski et al. 2010), although other studies propose post-Eocene delamination of the lithospheric mantle beneath the Dinarides as the main factor of the magma generation (e.g., Schefer et al. 2011; Balling et al. 2021). Apart from the Golija magmatic complex, I-type granitoids also occur and were paleomagnetically studied in the Kopaonik region (Lesić et al. 2013, 2019). A common feature of these plutons is the high degree of AMS anisotropy; however, there is a significant difference in the orientation of the AMS fabrics at the site level. The Golija pluton exhibits no preferred orientation (Table 1), while those from the Kopaonik area are characterised by well-defined magnetic foliation and lineation (Lesić et al. 2013), similarly to the younger Pohorje pluton, related to the Periadriatic shear zone (Márton et al. 2006; Fodor et al. 2020). The significant difference in the type of magnetic fabrics implies that the I-type granitoids (31.8–30.7 Ma, Schefer et al. 2011) of the Kopaonik region cooled down during active deformation, while the Golija intrusions (20.6–20.2 Ma, Schefer et al. 2011) in the absence of active deformation. The chaotic AMS fabric in the latter must have been governed by the viscous and slow-flowing magma (Tarling & Hrouda 1993). Oligocene dacitoandesites (32–30 Ma; Cvetković et al. 1995) of the Kopaonik region (Lesić et al. 2013) and quartz latites of the Golija complex (Table 1) are both characterized by a low degree of AMS with dominant foliation, indicating that during the formation of these rocks, there was no active deformation.

Paleomagnetic overall mean direction for the Miocene magmatic sites (excluding site M13) and the remagnetized Upper Cretaceous flysch localities suggest about a 30° CW vertical axis rotation (Fig. 7A, B). Remagnetization of the flysch is

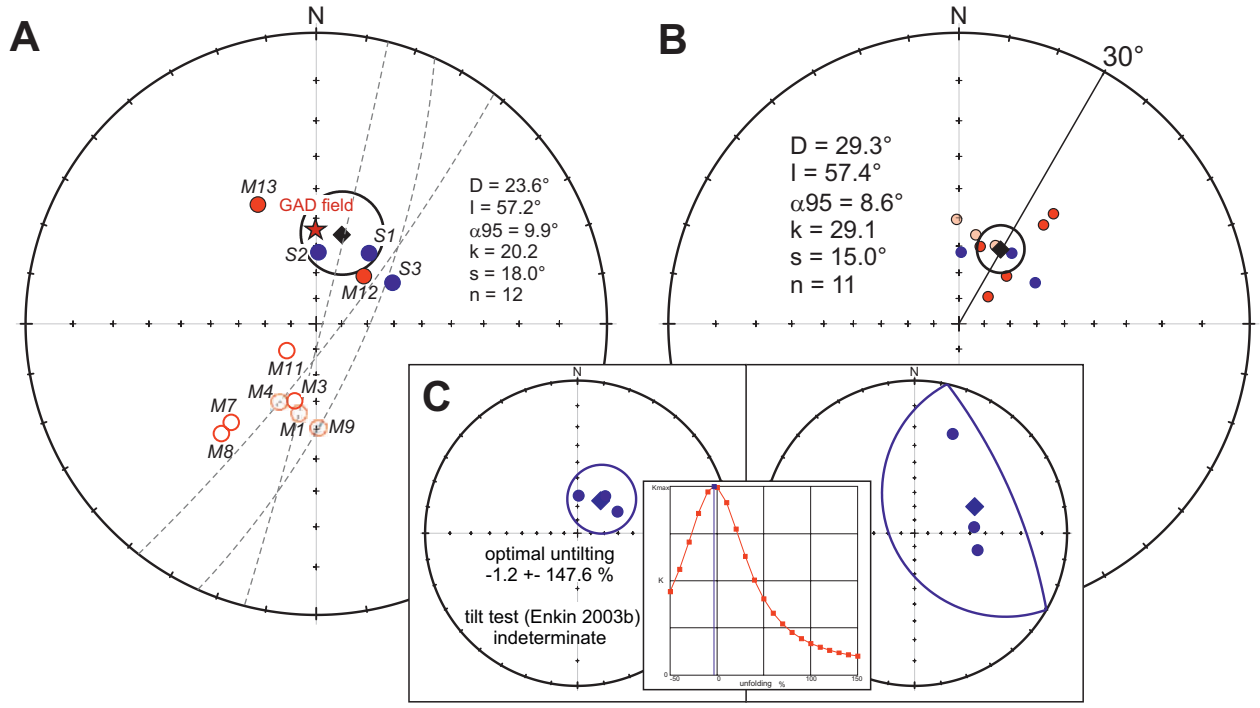

Fig. 7. A — Site mean directions (circles) and overall mean direction (black square with the respective α95) for Miocene igneous rocks (red) and remagnetized Campanian–Maastrichtian flysch (blue) on stereographic projection. Directions of sites M1, M4 and M9 were evaluated with combined great circle analysis (pink circles). Open circles represent negative inclinations; the red star represents the present-day geomagnetic field in the study area. **B** — Site mean directions and overall mean direction (all turned to normal polarity) after Watkins (1973) cut-off method. **C** — Mean directions of the flysch rocks before (left) and after (right) tilt correction. Tilt test result (Enkin 2003b) with the syn-tilting diagram is also shown. Key: D, I – declination and inclination of the overall mean direction; α95 and k – statistical parameters (Fisher 1953); s – angular standard deviation (Tauxe & Kent 2004); n – number of sites/localities.

supported by the well-clustered paleomagnetic directions before tilt correction with the same overall mean direction as the Miocene igneous rocks. While most of the magmatic sites have negative inclinations (Fig. 7A), all the flysch localities (situated close to site M12) have normal polarity mean directions. The presence of both polarity directions in our data set may account for the outlier direction (M13), which could have been acquired during polarity change of the magnetic field of the Earth, since this site was co-magmatic with the rest of the sites based on the thin section analysis.

The combined result of the Miocene magmatic rocks and the remagnetized flysch of the Drina–Ivanjica Unit (Table 4) is in a perfect fit with the earlier published paleomagnetic results of the adjacent Vardar Zone (Lesić et al. 2019; Márton et al. 2022b) obtained for Oligocene magmatic rocks from the Kopaonik region (Western Vardar Zone), Oligocene–Miocene extrusives and remagnetized Upper Cretaceous sediments from the Rudnik area (Western Vardar Zone), Oligocene dykes, and remagnetized Upper Cretaceous sediments from the Eastern Vardar Zone (Fig. 8). This implies a coordinated rotation for the Drina–Ivanjica Unit and the Vardar Zone; however, compared to the earliest possible time, 23 Ma (Márton et al. 2022b), the new results from the Drina–Ivanjica Unit added a new constraint, which is about 20 Ma for the commencement of the CW rotation (age of the Golija igneous rocks are 20.6–20.2 Ma; Schefer et al. 2011). For the upper age limit, 18–17 Ma is proposed, based on the strain field and AMS investigations of the Polumir pluton (U–Pb age; Schefer et al. 2011) from the Western Vardar Zone (Márton et al. 2022b). The rotation could have been triggered by the rollback effect of the Carpathian subduction, which also must have been responsible for the opening of the Pannonian Basin (Horváth 1993; Fodor et al. 1999; Matenco & Radivojević 2012; Toljić et al. 2013; Horváth et al. 2015; Márton et al. 2022b).

Paleomagnetic directions of the Upper Cretaceous sediments, which were studied from two basins far from the Golija magmatic complex, are well-clustered after tilt correction. In one, the Mokra Gora area, where the studied sediments are pelagic limestones, the result of the tilt test (Enkin 2003b) is positive (Table 4, Fig. 9A). For the other basin, near Zlatibor, the test is indeterminate with the optimal untilting at 50 % (Table 4, Fig. 9B), which can be attributed to the very weak magnetization of the platform carbonates and the small differences between the tilt angles of the beds. As the joint tilt test for the two basins (Table 4, Fig. 9C) is very close to a positive result, and the pre- and post-tilting declinations are very similar (D≈15°; Table 4) we interpret this declination as indicating a minor post-Early Cretaceous and pre-Miocene CCW rotation of the Drina–Ivanjica Unit, subtracting the post-20 Ma 30° CW rotation. Somewhat larger, post-40 Ma CCW rotation

Table 4: Overall mean paleomagnetic directions and overall mean paleomagnetic poles for the Drina–Ivanjica Unit. Key as for Table 3 for the paleomagnetic directions, but N is the number of localities. Lat, Lon – geographic coordinates of the poles (WGS84); K and A95 – statistical parameters for poles (Fisher 1953). Tilt-test classification is based on Enkin (2003b); reversal test classification is based on McFadden & McElhinney (1990). **Bold**: tectonically meaningful direction * M13 was excluded: Watkins (1973) cut-off. ** S19 was excluded: layers are in tectonic relationship with the surroundings.

	Paleomagnetic directions									Geodynamic interpretation	Fold/Tilt test; reversal test	Paleomagnetic poles based on localities			
	N	D°	I°	k	α95°	Dc°	Ic°	k	α95°		Optimal untilting and classification	Lat°	Lon°	K	A95°
Miocene magmatites *	8	**27.3**	**56.1**	**27.1**	**10.8**	–	–	–	–		–	–	–	–	–
Upper Cretaceous flysch	3	**35.6**	**60.7**	**27.9**	**23.8**	66.3	43.4	4.7	64.6		−1.2±147.6 % indeterminate	–	–	–	–
Miocene magmatites and remagnetized Upper Cretaceous flysch	11	**29.3**	**57.4**	**29.1**	**8.6**	–	–	–	–	**post-20 Ma 30° CW rotation**	reversal test: Rb	67.4	119.7	18.0	11.1
Cenomanian – Turonian *Mokra Gora area*	5	26.3	71.0	13.6	21.5	**4.3**	**49.0**	**29.4**	**14.3**		73.3±65.5 % positive	–	–	–	–
Cenomanian – Turonian *Zlatibor area*	4	13.8	56.7	74.1	10.7	**27.8**	**45.9**	**76.8**	**10.6**		51.5±201.7% indeterminate	–	–	–	–
Cenomanian – Turonian *Mokra Gora + Zlatibor area*	9	19.0	64.6	19.5	12.0	**15.1**	**48.2**	**30.6**	**9.5**	**15° CCW rotation between 90 and 20 Ma**	63.4±34.3 % indeterminate	69.1	159.6	24.1	10.7
Triassic–Jurassic sedimentary rocks ** (S18: tilt corrected direction was used for both calculations)	5	**338.9**	**54.9**	**68.5**	**9.3**	304.4	52.0	27.2	14.9	**35° CCW rotation between 150 and 90 Ma**	29.3±45.8 % negative	70.2	260.4	42.7	11.8

was postulated for the Central Vardar Zone (Márton et al. 2022b), based on the results of remagnetized Upper Cretaceous sediments. The mean paleolatitude fits with the expected paleolatitude in a position between Africa and stable Europe for this age (GAPWP, Torsvik et al. 2012), and the mean paleodeclination to the observed declination pattern (Márton et al. 2022b).

The Triassic–Jurassic cover strata of the Drina–Ivanjica Unit, which were deposited before the ophiolite obduction, are mostly situated in the Dinaric Ophiolite Belt (Dimitrijević 1997; Vasković & Matović 2010), forming the western part of the Drina–Ivanjica Unit. The pre-Cretaceous sedimentary outcrops are widespread; however, the numbers of the localities, which are suitable for paleomagnetic investigation, are limited due to the common occurrence of syn-sedimentary tectonics and slumping. Eventually, seven localities were sampled and six of them yielded well-defined paleomagnetic mean directions (Table 3). Layers from locality S19 were in tectonic relationship with its surroundings, and the mean direction of this locality is an outlier (Watkins 1973); therefore, S19 was excluded from the regional tectonic interpretation. The remaining localities have normal polarity magnetizations – four of them are well-clustered before tilt correction and one (S18) fits this cluster after correction (Fig. 10). We tentatively suggest that the remagnetization is connected to the ophiolite obduction (Late Jurassic–earliest Cretaceous), which heated up the underlying rocks (inverted P–T gradients, Karamata 1968). The paleodeclination of the overall mean direction (Table 4) is about 340°, which means a net CCW rotation of 20° with respect of the present north. However, it can be interpreted

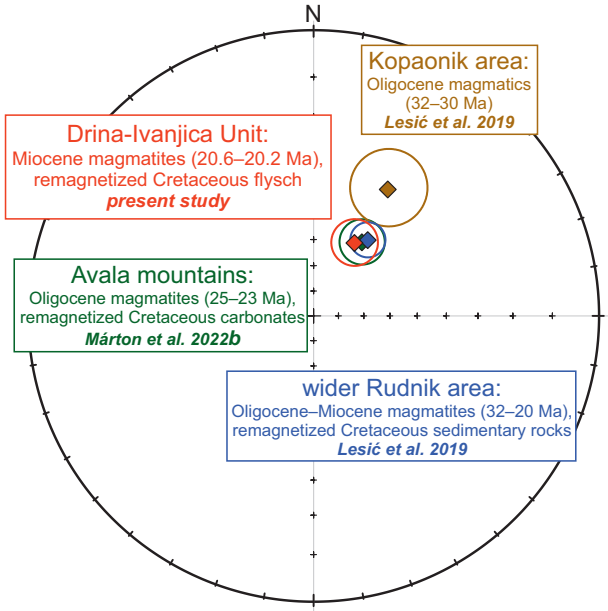

Fig. 8. Comparison between the Miocene overall mean direction of the Drina–Ivanjica Unit and the paleomagnetic directions of the earlier studied areas of the Vardar Zone (Avala Mts. – Eastern Vardar Zone; Kopaonik and Rudnik areas – Western Vardar Zone according to division of Toljić et al. 2019).

as a 50° CCW vertical axis rotation after 150 Ma and before the Miocene, considering the post-20 Ma 30° CW rotation. Part of this rotation must have taken place after the Late Cretaceous, as a 15° CCW rotation of the Drina–Ivanjica

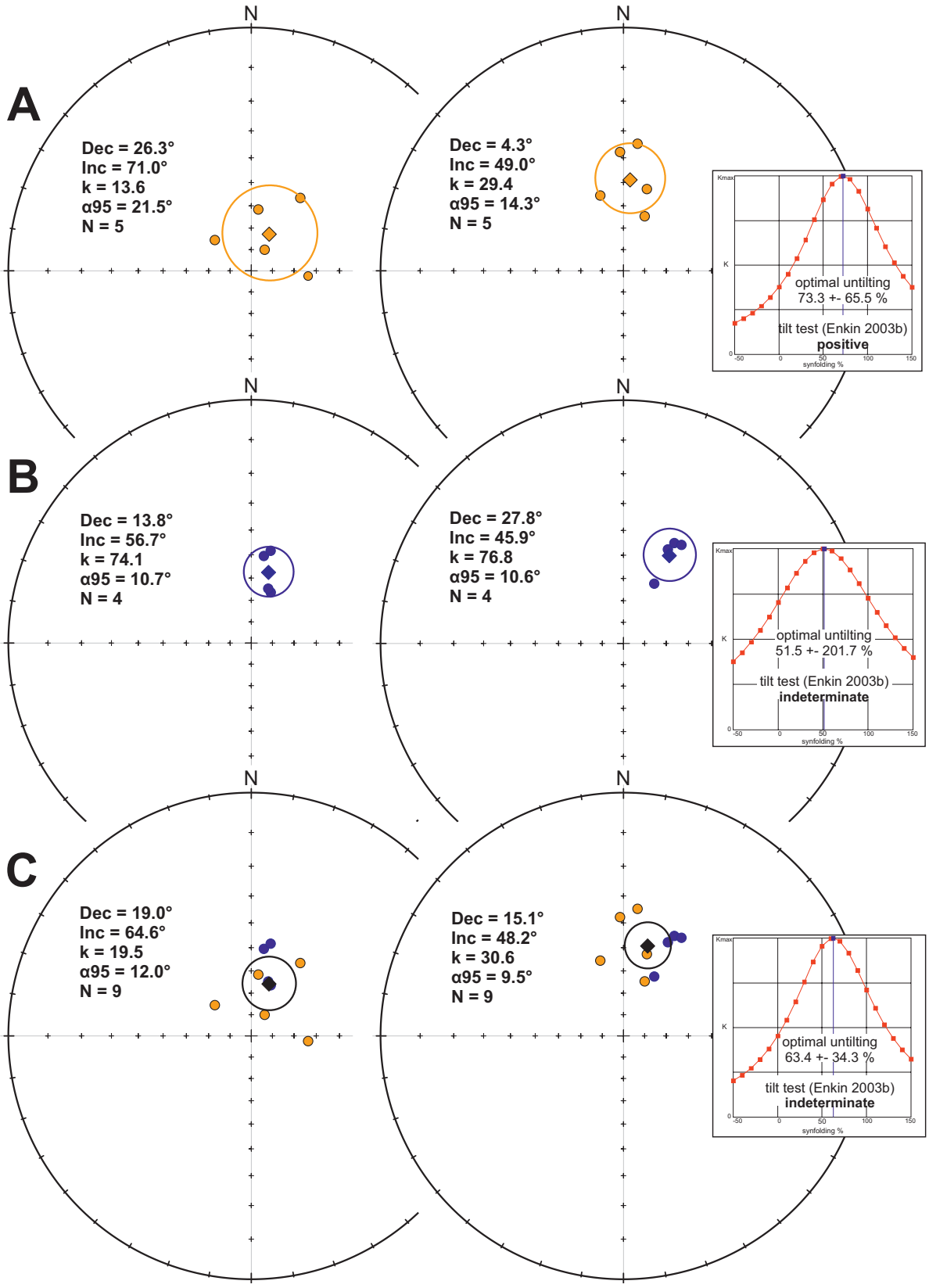

Fig. 9. Mean directions of the Cenomanian–Turonian sedimentary rocks before (left side) and after (right side) tilt correction. **A**, Mokra Gora area (gold symbols); **B** — Zlatibor area (blue symbols): indeterminate tilt-test is probably connected to the weaker magnetization and the small dip differences; **C** — combined results. Overall mean directions are plotted as squares with the respective α95. Tilt test results (Enkin 2003b) with syn-tilting diagrams are also shown in the right. Key as for Fig. 7.

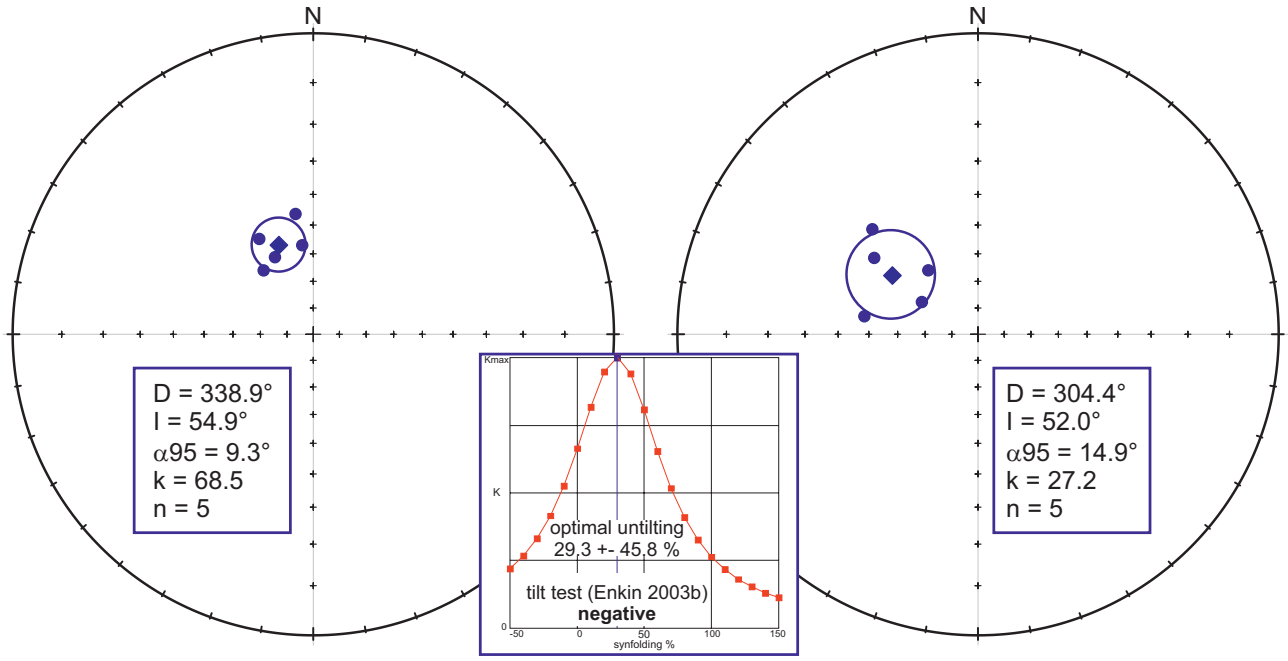

Fig. 10. Locality mean directions for Triassic–Jurassic sedimentary rocks of the Drina–Ivanjica Unit before (left side) and after (right side) tilt correction. Overall mean direction is shown as blue squares with the respective α95. Post-tilting direction was used for locality S18 for both overall mean direction calculations. Tilt test result (Enkin 2003b) with syn-tilting diagram is also shown in the middle. Key as for Fig. 7.

Unit between 90–20 Ma was interpreted for the Cenomanian–Turonian results. The post-150 Ma CCW rotation of the Drina–Ivanjica Unit is in line with the well-documented CCW rotation of the Adriatic microplate (Márton et al. 2017 and references therein), supporting the postulated Adriatic origin.

Conclusions

This paper presents the first paleomagnetic and AMS results, as well as their tectonic interpretation from the Drina–Ivanjica Unit of the Internal Dinarides. The results were obtained at 34 geographically distributed localities/sites (total of 358 drill cores oriented in situ) from the following groups of rocks: (1) Miocene Golija pluton and related extrusive igneous rocks, (2) Upper Cretaceous flysch sequences, which were thermally affected during the Miocene magmatic activity, (3) Upper Cretaceous post-obduction carbonate rocks of the Drina–Ivanjica Unit, and (4) Middle Triassic to Middle Jurassic limestones and marls representing the pre-obduction cover of the Drina–Ivanjica Unit.

The AMS measurements were practically confined to the igneous rocks, due to the very weak positive or negative susceptibilities in most of the studied sediments. The magnetic fabrics of the extrusive igneous rocks are rather weak and dominated by foliation. The Golija granodiorite is characterised by a high degree of anisotropy and no preferred orientation on the site level. This suggests that the pluton was intruded in the absence of active strain, unlike the older I-type and the younger S-type plutons of the Western Vardar Zone.

The products of the magmatic activity and the Upper Cretaceous flysch, which was clearly remagnetized during Miocene magmatism, point to a 30° CW rotation which must have taken place after 20 Ma. The angle and sense of the rotation suggests coordinated movement of the Drina–Ivanjica Unit with the adjacent Vardar Zone during the Miocene. Results of the present study set a younger age constraint (20 Ma) for the commencement of the CW rotation instead of the previously suggested 23 Ma. The rotation could be connected to the rollback effect of the Carpathian subduction, which initiated the formation of the Pannonian basin as well.

The paleomagnetic results from the post-obduction Late Cretaceous carbonates, which were sampled in two basins far away from the Golija pluton, are interpreted in terms of about 15° CCW rotation between the Late Cretaceous and 20 Ma, taking into consideration the 30° Miocene CW rotation.

The Triassic–Jurassic cover strata of the Drina–Ivanjica Unit yielded post-tilting magnetizations. The magnetizations were probably acquired during obduction of the ophiolites, suggesting about a 150 Ma age of magnetization acquisition. The overall mean direction indicates a total of 50° CCW rotation of the Drina–Ivanjica Unit between 150 Ma and the Miocene. This CCW rotation fits the paleomagnetically, well-documented post-150 Ma CCW rotation of Adria, and therefore supports the Adriatic affinity of the Drina–Ivanjica Unit.

Acknowledgements: The authors would like to thank Vladica Cvetković for the thin section analysis and the helpful comments, as well as László Fodor for the field work and geological observations at some of the sedimentary localities. The authors are also thankful to Uros Stojadinović and Jozef Madzin, who reviewed the manuscript. This work was supported by the ÚNKP-22-2 New National Excellence Program of the Ministry for Culture and Innovation from the source of the National Research, Development, and Innovation Fund and by the National Development and Innovation Office of Hungary, project K 128625, K 134873, and earlier K 113013. Field work was also supported by the "Contract on realisation and financing of scientific research of SRI in 2022", Nr. 451-03-68/2022-14/200126.

References

Alken P., Thébault E., Beggan C.D., Amit H., Aubert J., Baerenzung J., Bondar T.N., Brown W.J., Califf S., Chambodut A., Chulliat A., Cox G.A., Finlay C.C., Fournier A., Gillet N., Grayver A., Hammer M.D., Holschneider M., Huder L., Hulot G., Jager T., Kloss C., Korte M., Kuang W., Kuvshinov A., Langlais B., Léger J.M., Lesur V., Livermore P.W., Lowes F.J., Macmillan S., Magnes W., Mandea M., Marsal S., Matzka J., Metman M.C., Minami T., Morschhauser A., Mound J.E., Nair M., Nakano S., Olsen N., Pavón-Carrasco F.J., Petrov V.G., Ropp G., Rother M., Sabaka T.J., Sanchez S., Saturnino D., Schnepf N.R., Shen X., Stolle C., Tangborn A., Tøffner-Clausen L., Toh H., Torta J.M., Varner J., Vervelidou F., Vigneron P., Wardinski I., Wicht J., Woods A., Yang Y., Zeren Z. & Zhou B. 2021: International Geomagnetic Reference Field: the thirteenth generation. *Earth, Planets and Space* 73. https://doi.org/10.1186/s40623-020-01288-x

Balling P., Grützner C., Tomljenović B., Spakman W. & Ustaszewski K. 2021: Post-collisional mantle delamination in the Dinarides implied from staircases of Oligo-Miocene uplifted marine terraces. *Scientific Reports* 11, 2685. https://doi.org/10.1038/s41598-021-81561-5

Banjac J.N. 1994: Geology of the Upper Cretaceous of Mokra Gora (Western Serbia). *Univerzitet u Beogradu, Institut za regionalnu geologiju i paleontologiju*, 1–151.

Bernoulli D. & Laubscher H. 1972: The Palinspastic Problem of the Hellenides. *Eclogae Geologicae Helvetiae* 65, 107–118.

Bordás R. 1990: Aniso–anisotropy program package for IBM PC. *ELGI*, Budapest.

Borojević-Šoštarić S., Neubauer F., Handler R., Palinkaš A.L. 2012: Tectonothermal history of the basement rocks within the NW Dinarides: New $^{40}Ar/^{39}Ar$ ages and synthesis. *Geologica Carpathica* 63, 441–452.

Borojević-Šoštarić S., Palinkaš A.L., Neubauer F., Cvetković V., Bernroider M. & Genser J. 2014: The origin and age of the metamorphic sole from the Rogozna Mts., Western Vardar Belt: new evidence for the one-ocean model for the Balkan ophiolites. *Lithos* 192, 39–55.

Bortolotti V., Marroni M., Pandolfi L. & Principi G. 2005: Mesozoic to Tertiary tectonic history of the Mirdita ophiolites, northern Albania. *Island Arc* 14, 471–493.

Chadima M. & Jelínek V. 2008: Anisoft 4.2. – Anisotropy data browser. *Contributions to Geophysics and Geodesy* 38, 41.

Chiari M., Djerić N., Garfagnoli F., Hrvatović H., Krstić M., Levi N., Malasoma A., Marroni M., Menna F., Nirta G., Pandolfi L., Principi G., Saccani E., Stojadinović U. & Trivić B. 2011: The geology of the Zlatibor-Maljen area (western Serbia): A geotraverse across the ophiolites of the Dinaric-Hellenic collisional belt. *Ofioliti* 36, 2. https://doi.org/10.4454/ofioliti.v36i2.399

Ćirić B. 1958: Geologie des Gebiates fon Dragacevo (Westserbien). *Glasnik Prirodn. Muzeja, Serija A* 9, 5–159.

Cvetković V., Karamata S. & Knežević-Đorđević V. 1995: Volcanic rock of the Kopaonik area. [Savetovanje "Geologija I metalogenija Kopaonika"]. *Republički društveni fond za geološkaistraživanja Srbije*, 19–22 jun 1995, 185–195 (in Serbian with English abstract).

Cvetković V., Prelević D., Downes H., Jovanović M., Vaselli O. & Pécskay Z. 2004: Origin and geodynamic significance of Tertiary postcollisional basaltic magmatism in Serbia (central Balkan Peninsula). *Lithos* 73, 3–4. https://doi.org/10.1016/j.lithos.2003.12.004

Cvetković V., Prelević D. & Schmid S. 2016: Geology of South-Eastern Europe. In: Papic P. (Ed.): Mineral and Thermal Waters of Southeastern Europe. *Environmental Earth Sciences, Springer*, Cham. https://doi.org/10.1007/978-3-319-25379-4_1

Dimitrijević M.D. 1997: Geology of Yugoslavia. *Geoinstitut-Barex*, Beograd.

Dimitrijević M.N. & Dimitrijević M.D. 2009: The lower cretaceous paraflysch of the Vardar zone: Composition and fabric. *Annales geologiques de la Peninsule balkanique* 70. https://doi.org/10.2298/gabp0970009d

Dimo-Lahitte A., Monié P. & Vergély P. 2001: Metamorphic soles from the Albanian ophiolites: Petrology, $^{40}Ar/^{39}Ar$ geochronology, and geodynamic evolution. *Tectonics* 20, 78–96.

Djerić N., Gerzina N. & Schmid S.M. 2007: Age of the Jurassic radiolarian chert formation from the Zlatar mountain (SW Serbia). *Ofioliti* 32. https://doi.org/10.4454/ofioliti.v32i2.350

Enkin R. 2003a: PMGSC Paleomagnetism Data Analysis, v 4.2. *Geological Survey of Canada*, Sidney.

Enkin R. 2003b: The direction – correction tilt test: An all-purpose tilt/fold test for paleomagnetic studies. *Earth and Planetary Science Letters* 212. https://doi.org/10.1016/S0012-821X(03)00238-3

Fisher R. 1953: Dispersion on a Sphere. *Proceedings of the Royal Society A: Mathematical, Physical and Engineering Sciences* 217. https://doi.org/10.1098/rspa.1953.0064

Fodor L., Csontos L., Bada G., Győrfi I. & Benkovics L. 1999: Tertiary tectonic evolution of the Pannonian Basin System and neighbouring orogens: a new synthesis of palaeostress data. *Geological Society London Special Publications* 156, 295–334. https://doi.org/10.1144/GSL.SP.1999.156.01.15

Fodor L., Márton E., Vrabec M., Koroknai B., Trajanova M. & Vrabec M. 2020: Relationship between magnetic fabrics and deformation of the Miocene Pohorje intrusions and surrounding sediments (Eastern Alps). *International Journal of Earth Sciences* 109. https://doi.org/10.1007/s00531-020-01846-4

Gawlick H.J., Sudar M., Suzuki H., Derić N., Missoni S., Lein R. & Jovanović D. 2009: Upper Triassic and Middle Jurassic radiolarians from the ophiolitic mélange of the Dinaridic Ophiolite Belt, SW Serbia. *Neues Jahrbuch fur Geologie und Palaontologie – Abhandlungen* 253. https://doi.org/10.1127/0077-7749/2009/0253-0293

Gawlick H.J., Missoni S., Suzuki H., Sudar M.N., Lein R. & Jovanović D. 2016: Triassic radiolarite and carbonate components from a Jurassic ophiolitic mélange (Dinaric Ophiolite Belt). *Swiss Journal of Geosciences* 109, 473–494. https://doi.org/10.1007/s00015-016-0232-5

Gawlick H.J., Sudar M.N., Missoni S., Suzuki H., Lein R. & Jovanovic D. 2017: Triassic–Jurassic geodynamic history of the Dinaridic Ophiolite Belt (Inner Dinarides, SW Serbia). *Journal of Alpine Geology* 55, 1–167.

Halls H.C. 1978: The use of converging remagnetization circles in palaeomagnetism. *Physics of the Earth and Planetary Interiors* 16. https://doi.org/10.1016/0031-9201(78)90095-X

Horváth F. 1993: Towards a mechanical model for the formation of the Pannonian basin. *Tectonophysics* 226. https://doi.org/10.1016/0040-1951(93)90126-5

Horváth F., Musitz B., Balázs A., Végh A., Uhrin A., Nádor A., Koroknai B., Pap N., Tóth T. & Wórum G. 2015: Evolution of the Pannonian basin and its geothermal resources. *Geothermics* 53, 328–352. https://doi.org/10.1016/j.geothermics.2014.07.009

Hounslow M.W. 2006: PMagTools version 4.2 – a tool for analysis of 2-D and 3-D directional data. https://doi.org/10.13140/RG.2.2.19872.58880

Hrouda F. 1994: A technique for the measurement of thermal changes of magnetic susceptibility of weakly magnetic rocks by the CS-2 apparatus and KLY-2 Kappabridge. *Geophysical Journal International* 118, 604–612. https://doi.org/10.1111/j.1365-246X.1994.tb03987.x

Ilić A. & Neubauer F. 2005: Tertiary to recent oblique convergence and wrenching of the Central Dinarides: Constraints from a paleostress study. *Tectonophysics* 410. https://doi.org/10.1016/j.tecto.2005.02.019

Jelínek V. & Kropáček V. 1978: Statistical processing of anisotropy of magnetic susceptibility measured on groups of specimens. *Studia Geophysica et Geodaetica* 22. https://doi.org/10.1007/BF01613632

Karamata S. 1968: Zonality in contact metamorphic rocks around the ultramafic mass of Brezovica (Serbia, Yugoslavia). In: Proceedings of the 27th International Geological Congress. Prague, 1, 197–207.

Karamata S. 2006: The geological development of the Balkan Peninsula related to the approach, collision and compression of Gondwanan and Eurasian units. *Geological Society Special Publication* 260. https://doi.org/10.1144/GSL.SP.2006.260.01.07

Karamata S., Krstić B., Dimitrijević M.D., Knežević V., Dimitrijević M.N. & Filipović I. 1994: Terranes between the Adriatic and the Carpatho-Balkan Arc. *Bulletin CVIII de l'Acad. Serbe des Sciences et des Arts, Classe des Sciences Naturelles et Mathematiques* 35, 47–68.

Kirschvink J.L. 1980: The least-squares line and plane and the analysis of palaeomagnetic data. *Geophysical Journal of the Royal Astronomical Society* 62. https://doi.org/10.1111/j.1365-246X.1980.tb02601.x

Kossmat F. 1924: Geologie der zentralen Balkanhalbinsel, mit einer Übersicht des dinarischen Gebirgsbaus. In: Wilder J. (Ed.): Die Kriegsschauplätze 1914–1918 geologisch dargestellt. *Verlag Gebrüder Bornträger*, Berlin, 1–198.

Lesić V., Márton E., Cvetkov V. & Tomić D. 2013: Magnetic anisotropy of Cenozoic igneous rocks from the Vardar zone (Kopaonik area, Serbia). *Geophysical Journal International* 193. https://doi.org/10.1093/gji/ggt062

Lesić V., Márton E., Gajić V., Jovanović D. & Cvetkov V. 2019: Clockwise vertical-axis rotation in the West Vardar zone of Serbia: tectonic implications. *Swiss Journal of Geosciences* 112. https://doi.org/10.1007/s00015-018-0321-8

Lowrie W. 1990: Identification of ferromagnetic minerals in a rock by coercivity and unblocking temperature properties. *Geophysical Research Letters* 17. https://doi.org/10.1029/GL017i002p00159

Márton E. & Milićević V. 1994: Tectonically oriented paleomagnetic investigation in the Dinarids, between Zadar and Split. *Geophysical Transactions - Eotvos Lorand Geophysical Institute of Hungary* 39, 227–232.

Márton E. & Moro A. 2009: New paleomagnetic results from imbricated Adria: 1st island and related areas. *Geologia Croatica* 62. https://doi.org/10.4154/gc.2009.09

Márton E. & Veljović D. 1983: Paleomagnetism of the Istria peninsula, Yugoslavia. *Tectonophysics* 1. https://doi.org/10.1016/0040-1951(83)90058-6

Márton E. & Veljović D. 1987: Paleomagnetism of Cretaceous carbonates from the northwestern part of the Dinaric fold belt. *Tectonophysics* 134. https://doi.org/10.1016/0040-1951(87)90345-3

Márton E., Drobne K., Ćosović V. & Moro A. 2003: Paleomagnetic evidence for Tertiary counterclockwise rotation of Adria. *Tectonophysics* 377. https://doi.org/10.1016/j.tecto.2003.08.022

Márton E., Trajanova M., Zupančič N. & Jelen B. 2006: Formation, uplift and tectonic integration of a Periadriatic intrusive complex (Pohorje, Slovenia) as reflected in magnetic parameters and palaeomagnetic directions. *Geophysical Journal International* 167. https://doi.org/10.1111/j.1365-246X.2006.03098.x

Márton E., Ćosović V., Moro A. & Zvocak S. 2008: The motion of Adria during the Late Jurassic and Cretaceous: New paleomagnetic results from stable Istria. *Tectonophysics* 454. https://doi.org/10.1016/j.tecto.2008.04.002

Márton E., Ćosović V., Bucković D. & Moro A. 2010: New Cretaceous paleomagnetic results from the foreland of the Southern Alps and the refined apparent polar wander path for stable Adria. *Tectonophysics* 480. https://doi.org/10.1016/j.tecto.2009.09.003

Márton E., Zampieri D., Kázmér M., Dunkl I. & Frisch W. 2011: New Paleocene–Eocene paleomagnetic results from the foreland of the Southern Alps confirm decoupling of stable Adria from the African plate. *Tectonophysics* 504. https://doi.org/10.1016/j.tecto.2011.03.006

Márton E., Ćosović V. & Moro A. 2014: New stepping stones, Dugi otok and Vis islands, in the systematic paleomagnetic study of the Adriatic region and their significance in evaluations of existing tectonic models. *Tectonophysics* 611. https://doi.org/10.1016/j.tecto.2013.11.016

Márton E., Zampieri D., Ćosović V., Moro A. & Drobne K. 2017: Apparent polar wander path for Adria extended by new Jurassic paleomagnetic results from its stable core: Tectonic implications. *Tectonophysics* 700–701. https://doi.org/10.1016/j.tecto.2017.02.004

Márton E., Ćosović V., Imre G. & Velki M. 2022a: Changing directions of the tectonic structures, consistent paleomagnetic directions at the NE imbricated margin of Stable Adria. *Tectonophysics* 843. https://doi.org/10.1016/j.tecto.2022.229594

Márton E., Toljić M. & Cvetkov V. 2022b: Late and post-collisional tectonic evolution of the Adria-Europe suture in the Vardar Zone. *Journal of Geodynamics* 149. https://doi.org/10.1016/j.jog.2021.101880

Matenco L. & Radivojević D. 2012: On the formation and evolution of the Pannonian Basin: Constraints derived from the structure of the junction area between the Carpathians and Dinarides. *Tectonics* 31. https://doi.org/10.1029/2012TC003206

McFadden P.L. & McElhinney M.W. 1988: The combined analysis of remagnetization circles and direct observations in paleomagnetism. *Earth and Planetary Science Letters* 87, 161–172. https://doi.org/10.1016/0012-821X(88)90072-6

McFadden P.L. & McElhinney M.W. 1990: Classification of the reversal test in palaeomagnetism. *Geophysical Journal International* 103, 725–729. https://doi.org/10.1111/j.1365-246X.1990.tb05683.x

Milovanović D. 1984: Petrology of low metamorphosed rocks of the central part of the Drina–Ivanjica Paleozoic. *Bulletin du Muséum national d'Historie Naturelle,* Belgrade, A 39, 13–139.

Nirta G., Aberhan M., Bortolotti V., Carras N., Menna F. & Fazzuoli M. 2020: Deciphering the geodynamic evolution of the Dinaric orogen through the study of the "overstepping" Cretaceous successions. *Geological Magazine* 157. https://doi.org/10.1017/S001675682000045X

Osnovna Geološka Karta SFRJ: Geological maps of former Yugoslavia, 1:100.000, Beograd, Savezni Geoloski Zavod.

Pamić J., Tomljenović B. & Balen D. 2002: Geodynamic and petrogenetic evolution of Alpine ophiolites from the central and NW Dinarides: An overview. *Lithos* 65. https://doi.org/10.1016/S0024-4937(02)00162-7

Parma J., Hrouda F., Pokorný J., Wohlgemuth J., Suza P., Šilinger P. & Zapletal K. 1993: A technique for measuring temperature dependent susceptibility of weakly magnetic rocks. *EOS, Transactions of the American Geophysical Union*, Spring meeting 1993, 113.

Porkoláb K., Kövér Sz., Benkó Zs., Héja G.H., Fialowski M., Soós B., Spajić Gerzina N., Đerić N. & Fodor L. 2019: Structural and geochronological constraints from the Drina–Ivanjica thrust sheet (Western Serbia): implications for the Cretaceous–Paleogene tectonics of the Internal Dinarides. *Swiss Journal of Geosciences* 112. https://doi.org/10.1007/s00015-018-0327-2

Radoičić R. & Schlagintweit F. 2007: *Neomeris mokragorensis sp. Nov.* (Calcareous alga, Dasycladales) from the cretaceous of Serbia, Montenegro and the Northern calcareous Alps, (Gosau group, Austria). *Geoloski anali Balkanskoga poluostrva* 68. https://doi.org/10.2298/gabp0701039r

Schefer S., Cvetković V., Fügenschuh B., Kounov A., Ovtcharova M., Schaltegger U. & Schmid S.M. 2011: Cenozoic granitoids in the Dinarides of southern Serbia: Age of intrusion, isotope geochemistry, exhumation history and significance for the geodynamic evolution of the Balkan Peninsula. *International Journal of Earth Sciences* 100. https://doi.org/10.1007/s00531-010-0599-x

Schmid S.M., Bernoulli D., Fügenschuh B., Matenco L., Schefer S., Schuster R., Tischler M. & Ustaszewski K. 2008: The Alpine–Carpathian–Dinaridic orogenic system: Correlation and evolution of tectonic units. *Swiss Journal of Geosciences* 101. https://doi.org/10.1007/s00015-008-1247-3

Schmid S.M., Fügenschuh B., Kounov A., Matenco L., Nievergelt P., Oberhänsli R., Pleuger J., Schefer S., Schuster R., Tomljenović B., Ustaszewski K. & van Hinsbergen D. 2020: Tectonic units of the Alpine collision zone between Eastern Alps and western Turkey. *Gondwana Research* 78, 308–374. https://doi.org/10.1016/j.gr.2019.07.005

Sudar M. 1986: Triassic microfossils and biostratigraphy of the Inner Dinarides between Gučevo and Ljubišnja Mts., Yugoslavia. *Annales Géologiques de la Péninsule Balkanique* 50, Beograd, 151–394 (in Serbian with English summary).

Tarling D.H. & Hrouda F. 1993: The magnetic anisotropy of rocks. *Chapman & Hall*, London, New York, 1–218.

Tauxe L. & Kent D.V. 2004: A simplified statistical model for the geomagnetic field and the detection of shallow bias in paleomagnetic inclinations: Was the ancient magnetic field dipolar? In: Timescales Of The Paleomagnetic Field. *Geophysical Monograph Series* 145. https://doi.org/10.1029/145GM08

Toljić M., Matenco L., Ducea M., Stojadinović U., Milivojević J. & Derić N. 2013: The evolution of a key segment in the Europe–Adria collision: The Fruška Gora of northern Serbia. *Global and Planetary Change* 103. https://doi.org/10.1016/j.gloplacha.2012.10.009

Toljić M., Matenco L., Stojadinović U., Willingshofer E. & Ljubović-Obradović D. 2018: Understanding fossil fore-arc basins: Inferences from the Cretaceous Adria-Europe convergence in the NE Dinarides. *Global and Planetary Change* 171. https://doi.org/10.1016/j.gloplacha.2018.01.018

Toljić M., Stojadinović U. & Krstekanić N. 2019: Vardar Zone: NEW INSIGHTS INTO THE TECTONODEPOSITIONAL SUBDIVISION. In: Proceedings of the II Congress of Geologists of Bosnia and Herzegovina, October 2-4. Laktaši, Bosnia and Herzegovina, 60–73.

Torsvik T.H., Van der Voo R., Preeden U., Mac Niocaill C., Steinberger B., Doubrovine P.V., van Hinsbergen D.J.J., Domeier M., Gaina C., Tohver E., Meert J.G., McCausland P.J.A. & Cocks L.R.M. 2012: Phanerozoic polar wander, palaeogeography and dynamics. *Earth-Science Reviews* 114, 325–368. https://doi.org/10.1016/j.earscirev.2012.06.002

Trivić B., Cvetković V., Smiljanić B. & Gajić R. 2010: Deformation pattern of the Palaeozoic units of the Tethyan suture in the Central Balkan Penninsula: A new insight from study of the Bukulja-Lazarevac Palaeozoic unit (Serbia). *Ofioliti* 35, 31–32.

Ustaszewski K., Kounov A., Schmid S.M., Schaltegger U., Krenn E., Frank W. & Fügenschuh B. 2010: Evolution of the Adria-Europe plate boundary in the northern Dinarides: From continent-continent collision to back-arc extension. *Tectonics* 29. https://doi.org/10.1029/2010TC002668

Vasković N. & Matović V. 2010: Ophiolites of the Vardar Zone and Dinarides: Central and West Serbia. *Acta mineralogica-petrographica* 24, 1–55.

Watkins N.D. 1973: Brunhes epoch geomagnetic secular variation on Reunion Island. *Journal of Geophysical Research* 78. https://doi.org/10.1029/jb078i032p07763

Werner T., Lewandowski M., Vlahović I., Velić I. & Sidorczuk M. 2015: Palaeomagnetism and rock magnetism of the Permian redbeds from the Velebit Mt. (Karst Dinarides, Croatia): Dating of the early Alpine tectonics in the Western Dinarides by a secondary magnetization. *Tectonophysics* 651. https://doi.org/10.1016/j.tecto.2015.03.022

Zelic M., Levi N., Malasoma A., Marroni M., Pandolfi L. & Trivic B. 2010: Alpine tectono-metamorphic history of the continental units from Vardar zone: The Kopaonik Metamorphic Complex (Dinaric-Hellenic belt, Serbia). *Geological Journal* 45. https://doi.org/10.1002/gj.1169

Zijderveld J.D.A. 1967: AC Demagnetization of Rocks: Analysis of Results. In: Runcorn S.K., Creer K.M. & Collinson D.W. (Eds.): Methods in Palaeomagnetism. *Elsevier*, Amsterdam, 254–286.